AGU PUBLICATIONS

Geochemistry, Geophysics, Geosystems

RESEARCH ARTICLE
10.1002/2016GC006301

Key Points:
- The Aeolian Arc is characterized by some of the strongest along-arc geochemical variations worldwide
- New B-Be systematics suggest a melt component at the edges of the arc
- Geochemical signatures from the Aeolian Arc are more consistent with hot subduction systems (e.g., Cascades and Mexican Volcanic Belt)

Supporting Information:
- Supporting Information S1
- Table S1

Correspondence to:
E. Gazel,
egazel@vt.edu

Citation:
Zamboni, D., E. Gazel, J. G. Ryan, C. Cannatelli, F. Lucchi, Z. D. Atlas, J. Trela, S. E. Mazza, and B. De Vivo (2016), Contrasting sediment melt and fluid signatures for magma components in the Aeolian Arc: Implications for numerical modeling of subduction systems, *Geochem. Geophys. Geosyst.*, *17*, 2034–2053, doi:10.1002/2016GC006301.

Received 8 FEB 2016
Accepted 5 MAY 2016
Accepted article online 10 MAY 2016
Published online 17 JUN 2016

Contrasting sediment melt and fluid signatures for magma components in the Aeolian Arc: Implications for numerical modeling of subduction systems

Denis Zamboni[1,2], Esteban Gazel[1], Jeffrey G. Ryan[3], Claudia Cannatelli[2,4], Federico Lucchi[5], Zachary D. Atlas[3], Jarek Trela[1], Sarah E. Mazza[1], and Benedetto De Vivo[2]

[1]Department of Geosciences, Virginia Tech, Blacksburg, Virginia, USA, [2]Dipartimento di Scienze della Terra, dell'Ambiente e delle Risorse, Università di Napoli Federico II, Napoli, Italy, [3]Department of Geology, University of South Florida, Tampa, Florida, USA, [4]Department of Geology and Andean Geothermal Centre of Excellence, Universidad de Chile, Santiago, Chile, [5]Dipartimento di Scienze Biologiche, Geologiche e Ambientali, Alma Mater Studiorum, Università di Bologna, Bologna, Italy

Abstract The complex geodynamic evolution of Aeolian Arc in the southern Tyrrhenian Sea resulted in melts with some of the most pronounced along the arc geochemical variation in incompatible trace elements and radiogenic isotopes worldwide, likely reflecting variations in arc magma source components. Here we elucidate the effects of subducted components on magma sources along different sections of the Aeolian Arc by evaluating systematics of elements depleted in the upper mantle but enriched in the subducting slab, focusing on a new set of B, Be, As, and Li measurements. Based on our new results, we suggest that both hydrous fluids and silicate melts were involved in element transport from the subducting slab to the mantle wedge. Hydrous fluids strongly influence the chemical composition of lavas in the central arc (Salina) while a melt component from subducted sediments probably plays a key role in metasomatic reactions in the mantle wedge below the peripheral islands (Stromboli). We also noted similarities in subducting components between the Aeolian Archipelago, the Phlegrean Fields, and other volcanic arcs/arc segments around the world (e.g., Sunda, Cascades, Mexican Volcanic Belt). We suggest that the presence of melt components in all these locations resulted from an increase in the mantle wedge temperature by inflow of hot asthenospheric material from tears/windows in the slab or from around the edges of the sinking slab.

1. Introduction

The geochemical evolution of the Earth is inherently related to subduction as this process recycles crustal material back into the mantle. The release of slab-derived fluids and melts transports water and other elements in the mantle wedge during progressive subduction, and lowers the solidus, viscosity, and density of the mantle wedge triggering partial melting [e.g., *Gill*, 1981; *Tatsumi and Eggins*, 1995; *Schmidt and Poli*, 1998; *Elliott*, 2003; *Manning*, 2004; *Hermann et al*., 2006; *Syracuse et al*., 2010; *Spandler and Pirard*, 2013; *Pirard and Hermann*, 2014]. Element recycling via subduction directly influences the geochemical variability in the deep mantle and contributes to the formation of distinct mantle domains evident in intraplate volcanoes [*Zindler and Hart*, 1986; *Plank and Langmuir*, 1993; *Rudnick*, 1995; *Hofmann*, 1997; *Ryan and Chauvel*, 2014].

Compared to intraplate and mid-ocean ridge magmas, the typical arc geochemical signature is characterized by higher abundances of light rare earth elements (LREE) and large ion lithophile elements (LILE) relative to high field strength elements (HFSE). Overall, the contents of HFSE in arc magmas may vary depending on their relative incompatibility (e.g., moderately incompatibility of Zr, Hf; and highly incompatible element Nb, Ta) or by the presence of phases like rutile [e.g., *Foley et al*., 2000] that will hold those elements in the subducting slab. The arc signature depends on the composition and proportion of the different source components (subducting oceanic crust, the overlying sediment, and mantle) and the thermal regime of the subduction system will control the mineral phase stability and the solidus of the subducted material. Variations in these conditions define the stability of key potential mineral phases (e.g., rutile for Ti, Nb, and HFSE, garnet for HREE, phengite for LILE, zircon for Zr and Hf, allanite, monazite and apatite for Th, U, and REE) resulting in a slab-signal that will manifest differently in every arc depending

mainly on subduction temperature and secondary on the potential of extracting fluids or melts from the subducting slab [e.g., *Hermann*, 2002; *Hermann et al*., 2006; *Klimm et al*., 2008; *Hermann and Rubatto*, 2009; *Skora and Blundy*, 2010; *Avanzinelli et al*., 2012; *Martindale et al*., 2013; *Skora et al*., 2015].

Volcanic arcs are emplaced above subducting oceanic slabs [e.g., *Tatsumi*, 1989; *Hawkesworth et al*., 1993; *Stolper and Newman*, 1994; *van Keken et al*., 2011] and in some locations the arc is also accompanied by a back-arc basin spreading center, dominated by extensional stresses and adiabatic decompression melting that can also be influenced by fluids derived from the subducting plate (e.g., Marianas, Izu-Bonin, Tonga-Kermadec, South Sandwich) [*Elliott et al*., 1997; *Barry et al*., 2006; *Turner et al*., 2009; *Tollstrup et al*., 2010]. Such a tectonic scenario is also found in the southern Tyrrhenian Sea (Italy), where the Aeolian Volcanic Arc (focus of this study) and associated Marsili back-arc basin (Figure 1a) resulted from the subduction of the Ionian Plate under the Calabrian Arc [e.g., *De Astis et al*., 2003; *Ventura*, 2013; *Peccerillo et al*., 2013]. Current geochemical data for volcanic rocks from the southern Tyrrhenian Sea proximal to the Aeolian Islands highlight the coexistence of mid-ocean ridge basalts (MORB) (i.e., Vavilov basin), intraplate oceanic island basalts (OIB) (i.e., Ustica and Prometeo seamounts), and typical arc geochemical signatures (i.e., Marsili) [*Ellam et al*., 1989; *Beccaluva et al*., 1990; *Trua et al*., 2004, 2011; *Peccerillo*, 2005] as a result of the tectonic complexity of the region.

Although crustal assimilation can explain localized processes in the genesis of felsic magmas (e.g., record of anatexis process beneath Lipari) [*Di Martino et al*., 2010, 2011], the effects on trace elements and radiogenic isotope ratios have been demonstrated to be limited (e.g., high concentrations of incompatible elements act as a buffer for the incompatible element ratios and radiogenic isotopes variations) [*Peccerillo and Frezzotti*, 2015 and reference therein]. Thus the extreme variations in trace element and isotopic compositions within a single island and along the entire Aeolian volcanic front cannot be simply explained by crustal interactions [e.g., *Peccerillo et al*., 2013]. Current interpretations for the geochemical variability along this arc include differences in melt sources to regional variations in the degree of partial melting [*Ellam et al*., 1988; *Francalanci et al*., 1993; *De Astis et al*., 2000; *Peccerillo*, 2005; *Peccerillo et al*., 2013].

The sediment supply to the central Ionian Sea derives from outflow from the Adriatic Sea and Gulf of Taranto and turbidity flows of terrigenous sediment from both the African margin and Calabrian Arc [*Weldeab et al*., 2002]. Subducted sediments and altered oceanic crust components play an important role in arc magmatism worldwide [*Plank and Langmuir*, 1998] and there is a general consensus about the role of subducted components in the genesis of Aeolian magmas [*Ellam et al*., 1988; *Tonarini et al*., 2001; *Francalanci et al*., 2007; *Peccerillo et al*., 2013]. Nonetheless, it is still necessary to discriminate between the effects of subduction-derived fluids and melts, in order to better understand the role that the different subduction-zone contributors play in modifying the mantle wedge and their effects on the volcanic output [e.g., *Class et al*., 2000; *Saginor et al*., 2013; *Ryan and Chauvel*, 2014]. The goal of this study is to investigate which slab-derived components (i.e., slab fluids or melts derived from the subducting crust and/or sediments) control the extreme along-arc variations in the geochemical signatures of Aeolian magmas in a west-east section of the arc from the island of Alicudi to Stromboli (Figure 1). We did not include the islands of Vulcano and Lipari in this study as the isotopic signature of lavas from these islands clearly points toward a lithospheric component [*De Astis et al*., 2013; *Forni et al*., 2013]. For this purpose, we report new B, Be, Li, As data as well as whole rock major and trace element compositions for olivine bearing mafic lavas, representative of primitive magmas largely unaffected by crustal contamination [e.g., *De Astis et al*., 2000; *Peccerillo*, 2005].

1.1. Geologic and Tectonic Background

The Aeolian Archipelago is located in the southern Tyrrhenian Sea, north of the Sicilian coast and west of the Calabrian Orogenic Arc (Figure 1a). It includes the islands of Alicudi, Filicudi, Salina, Lipari, Vulcano, Panarea, and Stromboli, and several seamounts around the Marsili oceanic basin (Figure 1b). The islands and seamounts depict a volcanic arc, which has been subdivided into three segments (western, central, and eastern) based on distinct volcanic and structural evidence [*De Astis et al*., 2003 and references therein; *Ventura*, 2013]. The western segment consists of Alicudi and Filicudi islands and the seamounts to the west, with the magma rising mainly controlled by the WNW–ESE Sisifo-Alicudi Fault System (SA) (Figure 1b) [*Ventura*, 2013 and reference therein]. The volcanism in this segment comprises some of the most primitive lavas of the entire arc with Mg-numbers (molar [MgO/[MgO+FeO]]*100) up to 73 in equilibrium with the mantle [*Peccerillo et al*., 2004]. This segment is currently inactive due to compressional stresses operating

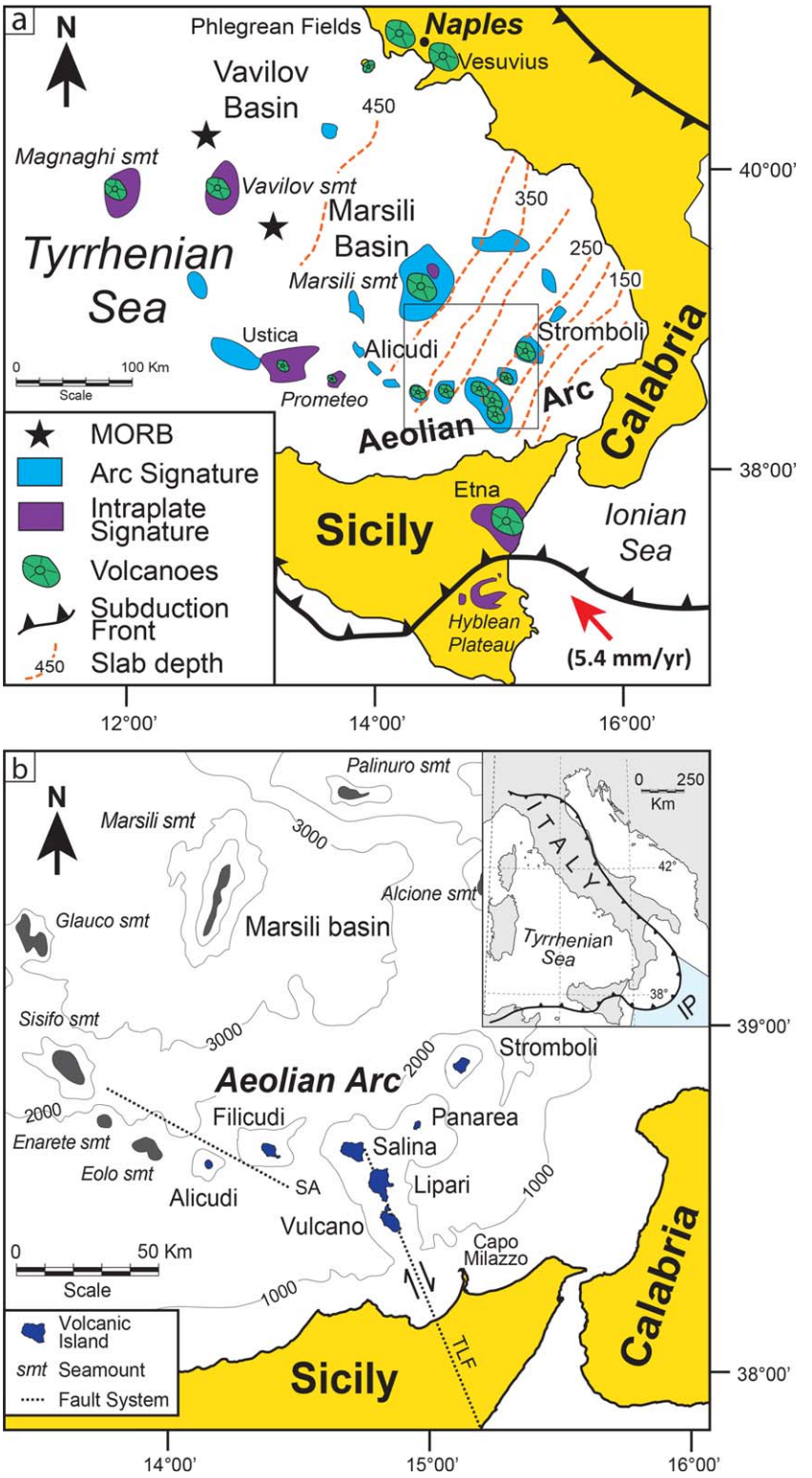

Figure 1. Tectonic setting and geochemical signatures of volcanic rocks of the southern Tyrrhenian Sea (Italy). (a) The dominant magma signatures of the main volcanoes are displayed along with the front of the Apennine-Maghrebid fold-and-thrust belt of the central Mediterranean region [after *Trua et al.*, 2007]. The depth contours of the Wadati-Benioff zone from *Faccenna et al.* [2011] are represented with orange-dashed lines. The red arrow is a geodetic vector representing the rate of subduction [*Faccenna et al.*, 2011]. (b) Geomorphology and bathymetric features of the Aeolian Arc and surrounding seamounts in the Marsili Basin (modified from *Peccerillo et al.* [2013]). The entire subduction/collision front is represented in the inset map of Italy. Abbreviations: IP = Ionian Plate; SA = Sisifo-Alicudi Fault System; Smt = seamount; TLF = Tindari-Letojanni Fault System.

west of the NNW–SSE Tindari-Letojanni Fault System (TLF) (Figure 1b) that appear to limit magma ascent [*Peccerillo et al*., 2004; *Ventura*, 2013]. The central arc segment includes the NNW-aligned Salina, Lipari, and Vulcano islands that are all affected by the TLF (Figure 1b), which produces transtensional stresses [*Ventura*, 2013]. The eastern arc segment comprises the islands of Panarea and Stromboli (and the seamounts to the north-east) that are strongly influenced by a prevailing NNE–SSW to NE–SW striking fault system responsible for the elongation of dikes and eruptive fissures [*Ventura*, 2013].

The basement of the Aeolian Arc consists of the Calabrian-Peloritan tectonic terrains (Calabria block) [*Rottura et al*., 1991] related to the European continental plate. The thickness of the continental crust varies from ~25 km, under the Calabrian Arc and the western Aeolian Islands, to 10 km, in the Marsili Basin [*Piromallo and Morelli*, 2003]. The occurrence of deep-focus earthquakes beneath the eastern segment of the Aeolian Arc defines the presently active subduction zone [*Falsaperla et al*., 1999; *Panza et al*., 2003, 2004]. Melting of the mantle wedge above the steep (~70°) north-west dipping, and rolling-back Ionian slab under the Calabrian Arc is responsible for the Aeolian volcanism [*Gvirtzman and Nur*, 2001; *Chiarabba et al*., 2008]. The oldest known volcanic activity in the area was ~1.3 Ma submarine volcanism at the Sisifo Seamount [*Beccaluva et al*., 1982], while the Eolo and Enarete seamounts around the Marsili Basin range between 850 and 640 ka in age [*Beccaluva et al*., 1985]. The subaerial volcanic activity began in Salina, Filicudi, and Lipari around 250–270 ka [*Forni et al*., 2013; *Lucchi et al*., 2013a, 2013b] and continues at present time in the central-eastern segments of the arc (Stromboli and Vulcano) above or at the margins of the deep seismicity zone [*Panza et al*., 2003].

Geochemical studies on the Marsili Seamount [*Trua et al*., 2007, 2011] suggest a compositional variation from a dominant arc signature to a younger, sporadic intraplate signature, geochemically similar to the Etna-Hyblean Plateau and related to the African mantle source [*Trua et al*., 2003]. Because of similarities in isotopic and trace element compositions between Alicudi lavas and the intraplate Marsili lavas [*Trua et al*., 2004, 2011], several authors proposed that the western segment of the Aeolian Arc includes some contribution of asthenospheric flow from the northern African mantle into the southern Tyrrhenian mantle wedge around the edges of the subducting Ionian slab [*Trua et al*., 2003, 2011; *Chiarabba et al*., 2008]. *De Astis et al*. [2006] also hypothesized that a similar mantle flow from the northeastern side of the slab might be responsible for the alkaline volcanism of Vesuvius and Stromboli. Additionally, *Peccerillo* [2001] proposed that the eastern segment of the Aeolian Islands might extend to Vesuvius and the Phlegrean Fields, based on compositional affinities (radiogenic isotopes and incompatible element ratios) between the Campanian Province lavas and Stromboli potassic rocks; although U-series disequilibria suggest the possibility of different metasomatizing components for Stromboli and Vesuvius [*Voltaggio et al*., 2004; *Tommasini et al*., 2007; *Avanzinelli et al*., 2008].

2. Materials and Methods

We collected mafic samples on the islands of Alicudi, Filicudi, Salina, and Stromboli based on previous studies [e.g., *Francalanci et al*., 2013; *Lucchi et al*., 2013a, 2013b, 2013d] that suggested that the units collected are not only the most mafic but also they do not show any important evidence of crustal contamination. *Peccerillo and Frezzotti* [2015] demonstrated that samples with MgO $\geq$ 3.5 wt. % do not show significant evidence of crustal interaction in their incompatible elements ratios and radiogenic isotope signatures. Based on this, we revisited outcrops of these well-characterized units and collected samples from olivine-bearing scoria and lavas with the goal of elucidating the effects of subducted components on the magma sources and avoiding any significant crustal contamination signatures. GPS locations are reported in supporting information Table S1A. For additional geologic background, *Lucchi et al*. [2013c] presents a comprehensive geologic description and history of the Aeolian archipelago and the units selected for this study.

All the samples were processed in the geochemistry laboratory at the Department of Geosciences at Virginia Tech. Rock sample preparation and analytical work were conducted following the procedures described in *Mazza et al*. [2014]. Major element composition were determined on rock powders fluxed into homogeneous glass fusion disks with a combination of $Li_2B_4O_7$ $LiBO_2$-LiBr from Spex® (certified $\ll$1 ppm blank for all trace elements) and analyzed with X-ray fluorescence (XRF) at Virginia Tech. For the major elements, the relative standard deviation (RSD) for 10 replicates of BHVO-2, run as an unknown, was <1% for all major elements while for AGV-2, run as unknown, was <1% with accuracy better than 2%. Additional

trace element compositions for samples of Stromboli were collected at Virginia Tech by laser ablation inductively coupled plasma mass spectrometry (LA-ICP-MS) in the same fusion disks with an Agilent 7500ce ICPMS coupled with a Geolas laser ablation system, with a He flow rate of ~1 L/m−5 Hz and an energy density on sample ~7–10 J/cm^2. Data were calibrated against USGS standards BHVO-2, BCR-2, BIR-1a, and G-2, using Ti from XRF as an internal standard and the standard element values reported in *Kelley et al*. [2003]. The accuracy for 10 replicates of BHVO-2 run as an unknown was better than 6% for all elements except for V, Cr, Sr, Nb, Ba, Eu, Lu, and Ta (7–9%) and Cs (10%), with RSD (1σ) better than 5% except for Cu, Zn, and Pb (7–9%) and Cs (12%). Trace elements contents from the island of Alicudi, Filicudi, and Salina were determined by solution ICP-MS at the USF Center for Geochemical Research at the University of South Florida together with Be and Li contents (also for Stromboli). Sample preparation for ICP-MS follows the analytical method described by *Kelley et al*. [2003], with sample dissolution by HF-HNO_3 digestion, using distilled acids. Data were calibrated against natural standard reference materials USGS CRM BHVO-2, BIR-1, BCR-2, NBS-688, and GSJ (Geological Survey of Japan) CRM JA-2 prepared as above. Accuracy was determined using GSJ standard JB-3 with RSD (1σ) for 4 replicates <5% for all elements. Errors on the analyses were generally 6% on Be and better than 10% on Li.

Boron and arsenic contents were determined by solution ICP-MS at the Center for Geochemical Analysis at the University of South Florida. Methods were modified from *Ryan and Langmuir* [1993] as follows: 0.5 g of each sample was mixed with 2 g of Na_2CO_3 flux (>99.9% purity) in 20 mL Pt crucibles. The covered crucibles were heated in a muffle furnace to 1050°C (conditions that are not reducing enough to make element compounds that are volatile under fusion conditions, like As hydrides), and then cooled to room temperature. The cooled crucibles were immersed in 80 mL of de-ionized mannitol distilled B-free water 180 mL Savillex jars, sealed and placed on a hot plate at 100°C for 12 h. Boron and arsenic are separated as part of the water-soluble fraction of the fusion cake (compose of highly water soluble but poorly volatile oxides), along with the heavier alkali metals; other species remain sequestered in the water-insoluble portion. The fusion cakes were extracted from the crucibles with Teflon spatulas, and rinsed profusely in B-free DI water. The resulting solution was evaporated to ~20 mL total volume. These solutions were then decanted, rinsed, and centrifuged for 15 min to separate the insolubles. Supernates were collected in Savillex jars, dried, and resuspended in 20 mL of B-free water and 5 mL of distilled HNO_3. The acidified solutions were allowed to sit at room temperature for several hours for SiO_2 to precipitate, and were then centrifuged to separate silica, and diluted to 50 g total solution weight using de-ionized B-free water, centrifuged to separate silica, and decanted to 15 mL centrifuge tubes for analysis.

Fluid mobile element (FME) solutions were analyzed on a Perkin Elmer Elan DRC II Q-ICPMS using a PFA teflon front end attached to a pure quartz concentric spray chamber. Since the potential for contamination by boron in glass is high, blanks were repeatedly run to ensure that there was no contamination from the sample introduction system. Analytical conditions on the ICP were standard mode for all elements (including As) and tuning was performed by standard routines with special emphasis on low mass elements. Since no chloride matrix was present, there was no potential for ArCl interference at mass 75; which was confirmed by our blank analysis. Calibration curves were obtained using a series of natural standard reference materials (USGS CRM BHVO-2, BIR-1, BCR-2 and GSJ CRM JA-2) prepared in the same manner as samples. Accuracy and precision were referenced against GSJ CRM JB-3 using SRM ANRT-DRN as a drift standard (which also provides an additional check of accuracy) also prepared as before. Reproducibility of the As and some of the other FME (Cs and Rb) measured in the HF-HNO_3 solution confirm our results from the Na_2CO_3 fusion fluxed method. Accuracy and precision was generally 9% or better on B and close to 6% on As as obtained by replicate analysis of the reference material JB-3. Additionally Rb, Cs, Sr, and Ba were analyzed by this method with good reproducibility on JB-3. Samples were analyzed as duplicates during the analysis and reproducibility on Boron was better than 8% and better than 6% on sample replicates (supporting information Table S1B).

3. Results

The samples collected for this study range in composition from calc-alkaline to high potassium basalt to andesite. The samples are characterized by porphyritic texture with variable phenocryst content. When plotted in the classic SiO_2 versus K_2O diagram from *Peccerillo and Taylor* [1976], our new data (supporting

information Table S1C) have compositions in agreement with previously collected major element data (Figure 2). In the western segment of the Aeolian Arc (Figure 2a), samples from Alicudi vary from basalt to andesite and plot in the calc-alkaline and high potassic calc-alkaline fields. Most of the Filicudi samples are basalts that plot near the boundary between the calc-alkaline and high potassic calc-alkaline series. Samples from Salina in the central arc segment (Figure 2b) are calc-alkaline basalts, and basaltic-andesites. In the eastern arc segment, Stromboli displays an important separation between lavas with high potassium contents ($K_2O > 3.5$ wt. %) that belong to the potassic series and other samples that plot in a range between the calc-alkaline and shoshonitic series (Figure 2c), in agreement with the compositional behavior described by *Francalanci et al*. [2013]. Major element trends are consistent with observed mineral phases in the samples that evidence the cotectic crystallization of olivine and clinopyroxene typical of wet arc magmas, characterized by an overall decreasing CaO and MgO and increasing Al_2O_3 during fractionation [e.g., *Zimmer et al*., 2010].

Our new B, Be, Li, and As data are reported in supporting information Table S1D and average values are plotted in Figures 3a, 3b, 3c, 3d to highlight the regional variations of these elements along the volcanic front. The Aeolian Arc shows varying B abundances, increasing from west to east, with Alicudi and Filicudi characterized by the lowest average B contents (∼7 ppm) and Stromboli showing the highest (∼19 ppm). The highest B content (30.3 ppm) is displayed by Stromboli calc-alkaline rocks. Samples from Salina and Filicudi have the lowest average Be concentrations (∼1 ppm), while Alicudi and Stromboli samples have the highest (∼2 and ∼4 ppm, respectively). More in details, Stromboli calc-alkaline rocks average ∼2 ppm while the potassic ones have an average ∼6 ppm. The maximum Be contents in the range 4.9–7.2 ppm are found in the potassic rocks of Stromboli and are ∼5 times greater than any other island in the Aeolian Arc. Lithium and arsenic contents vary similarly to B, with a general increasing from west to east along the arc with the highest values in Stromboli. However the variations in Li (and As) are not perfectly uniform with a gradual increase toward east, in fact Filicudi samples, for either Li and As, are characterized by the lowest average values (∼6 and ∼1 ppm, respectively). The average Li and As budgets of Alicudi and Salina are similar (∼8 and ∼2 ppm, respectively) while Stromboli has the highest. When fluid mobile elements (B, As and Li) are plotted against Be, there is a clear bimodal behavior with distinct trends for the calc-alkaline rocks and the potassic samples of Stromboli (Figures 3e, 3f, 3g).

4. Discussion

Magmas from the Aeolian Arc display some of the largest along-arc geochemical variations in the world [e.g., *Peccerillo*, 2005; *Peccerillo et al*., 2013]. This is particularly evident in the significant change in $^{87}Sr/^{86}Sr$ and $^{143}Nd/^{144}Nd$ isotopes ratios in less than 90 km along the volcanic front, from Alicudi to Stromboli (Figure 4). Current interpretations [*Francalanci et al*., 2007; *Peccerillo et al*., 2013] suggest that this signature is controlled by a depleted mantle source at Alicudi with an increasing role for subduction components or crustal contamination from west to east (Figure 4). Crustal contamination cannot account for the entire geochemical variation along the arc [*Ellam and Harmon*, 1990; *Peccerillo et al*., 2004, 2013] as it requires unrealistic extents of assimilation (up to 40% of average Calabrian crust) while at the same time maintaining a primitive basaltic composition in the erupted material [*De Astis et al*., 2000; *Peccerillo*, 2005]. *Peccerillo et al*. [2013] presented additional isotopic evidence of the source composition controlling the geochemical signature in the Aeolian Islands. These authors described how combination of O- and Sr-isotope studies is a powerful tool to discriminate magma-lithospheric interaction from source composition processes, concluding that variations in $^{87}Sr/^{86}Sr$ along the volcanic front is a direct manifestation of variations of source composition in the Aeolian Arc. Therefore, the regional geochemical trends recorded in the mafic lavas in the Aeolian Arc are most likely controlled by the addition of subduction components to the mantle wedge in the form of fluids and/or melts.

Fluids and melts derived from subducting sediments and oceanic lithosphere are known to be responsible for the chemical and rheological modification of the mantle wedge in subduction systems [e.g., *Ryan and Langmuir*, 1993; *Elliott et al*., 1997; *Johnson and Plank*, 1999; *Kelemen et al*., 2003; *Eiler et al*., 2005; *Kimura and Stern*, 2008; *Gazel et al*., 2009; *Hermann and Rubatto*, 2009; *Saginor et al*., 2013; *Martin et al*., 2014; *Gazel et al*., 2015]. At higher P-T conditions, the distinction between fluids and melts may not be possible if the system reaches a supercritical fluid phase [*Manning*, 2004; *Kessel et al*., 2005; *Pirard and Hermann*, 2014].

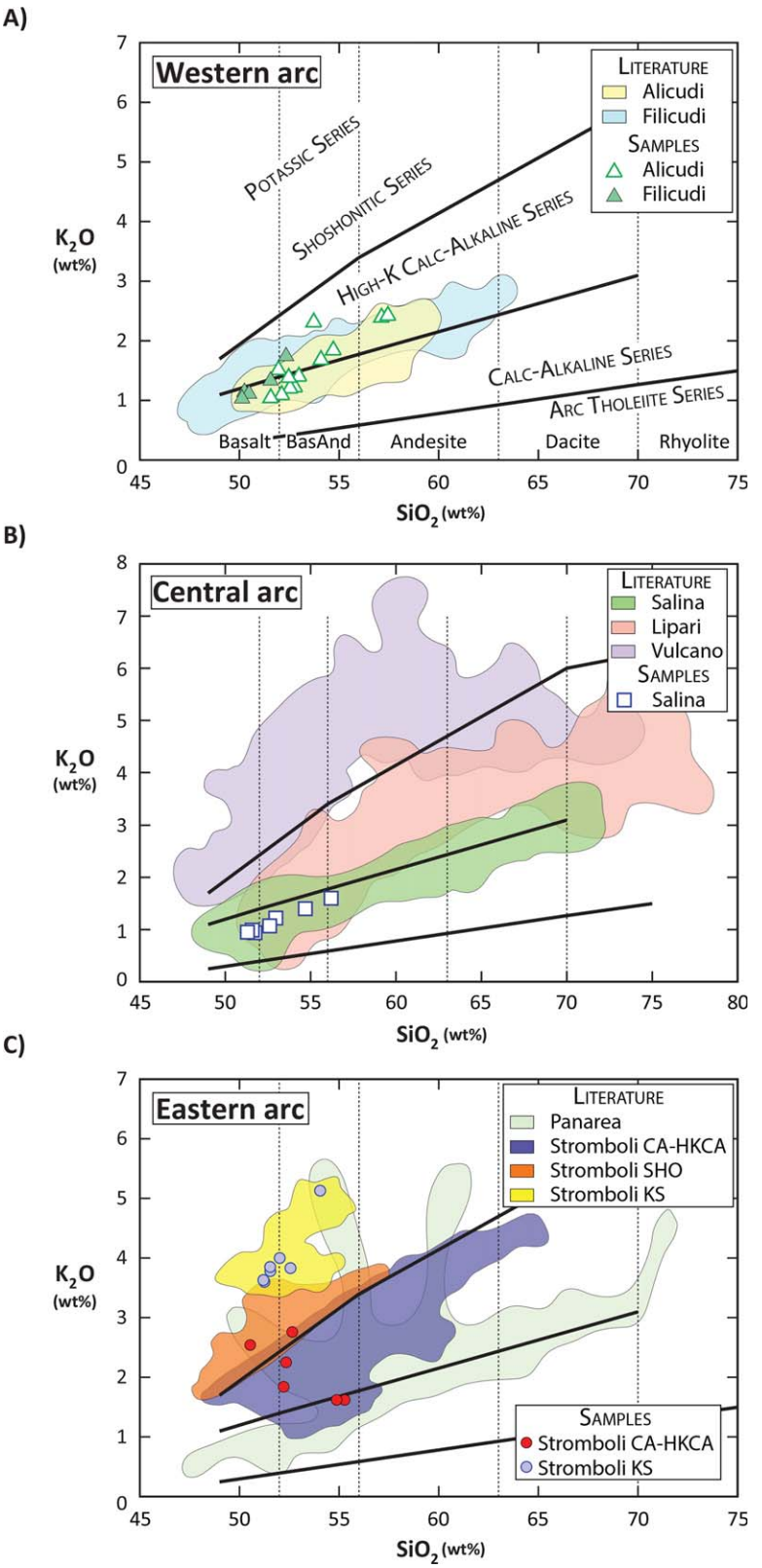

Figure 2. K_2O versus SiO_2 geochemical classification after *Peccerillo and Taylor* [1976] for the volcanic rocks of the Aeolian Arc showing our new samples compared with previous data collected in these islands from the compilation of *Lucchi et al*. [2013c].

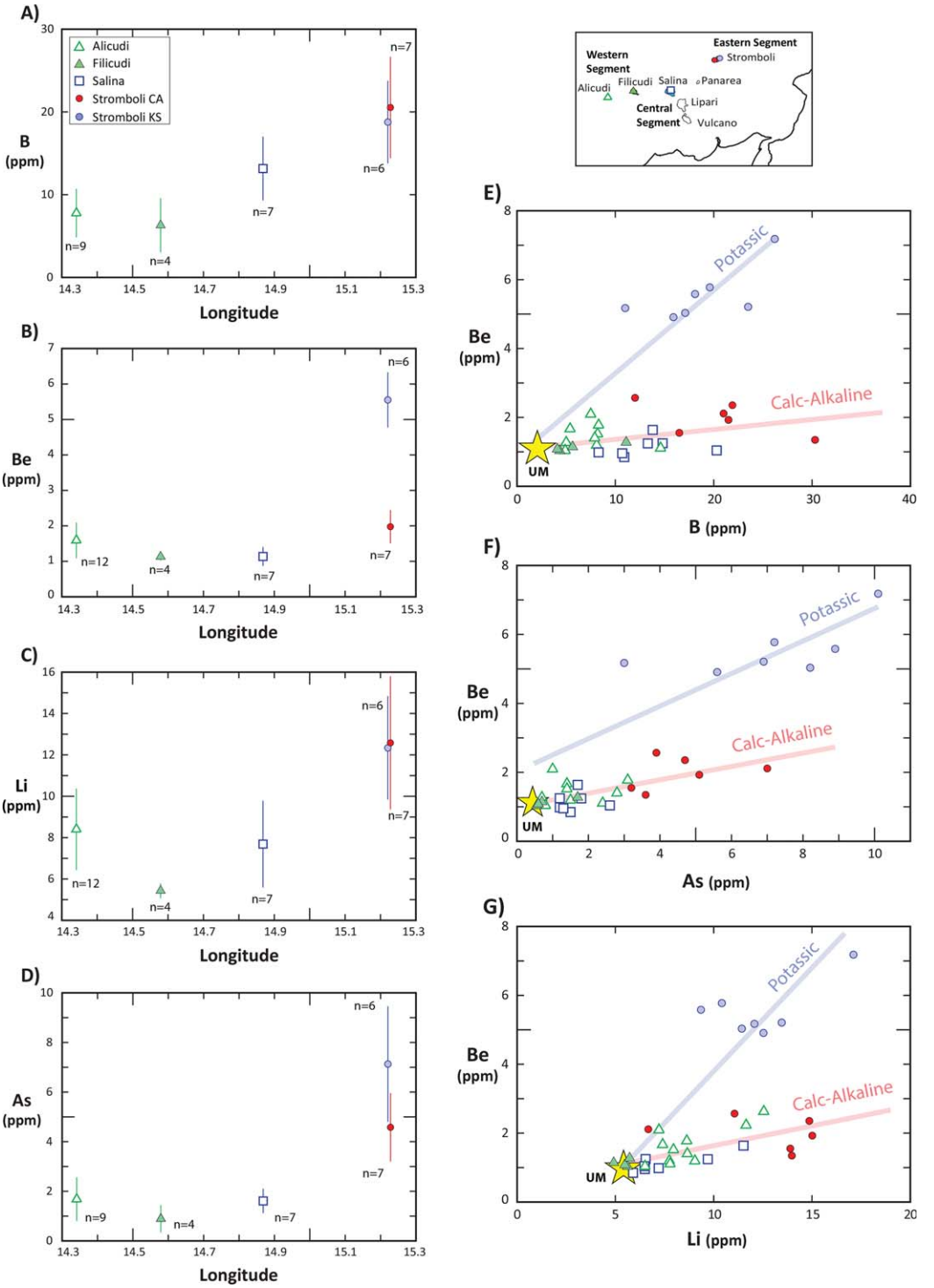

Figure 3. Regional along-arc variations of B (a), Be (b), Li (c), and As (d) for the Aeolian volcanic rocks collected in this study. Note the two trends between the calc-alkaline and potassic units in (e), (f), and (g) with respect to the average B, Be, Li, and As contents in the upper mantle (UM) derived melts. Those trends represent linear regression. R^2 for calc-alkaline and potassic trends: (e) 0.17 and 0.86, (f) 0.44 and 0.72, (g) 0.40 and 0.78. Upper mantle melts consist of MORB values from *Gale et al.* [2013] and *White and Klein*, [2014], and OIB values from *Ryan et al.* [1996b] and *Krienitz et al.* [2012]. No significant studies qualitatively measure As in MORB or intraplate magmas, thus we assume that the composition of these melts will plot at the convergence of the two trends as evident in the other elements. Vertical bars are the 1σ standard deviation of the range of the data; n = number of samples.

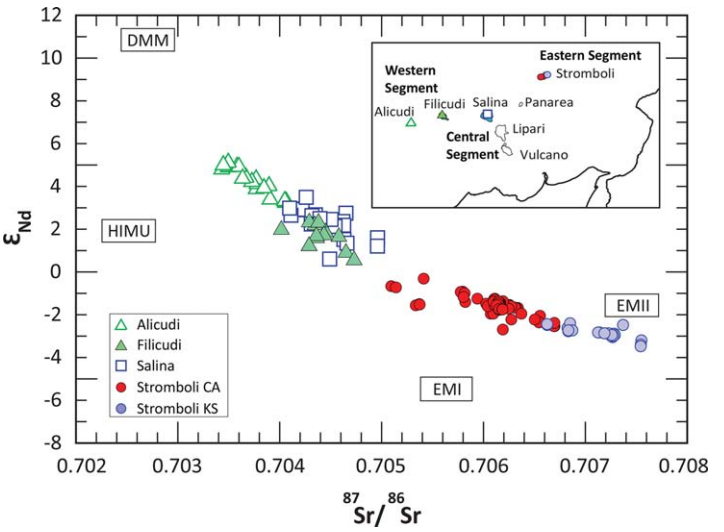

Figure 4. Regional variations of $^{87}Sr/^{86}Sr$ and $^{143}Nd/^{144}Nd$ (ε_{Nd}) in the Aeolian Arc from literature data. Note the decrease in $^{143}Nd/^{144}Nd$ and dramatic increase in $^{87}Sr/^{86}Sr$ from the western arc segment (Alicudi) to the eastern one (Stromboli) along a distance less than 90 km. Data compiled from: Alicudi, *Peccerillo and Wu* [1992]; *Peccerillo et al.* [1993, 2004]. Filicudi, *Francalanci and Santo* [1993]; *Santo* [2000]; *Santo et al.* [2004]. Salina, *Ellam* [1986]; *Ellam et al.* [1988, 1989]; *Ellam and Harmon* [1990]; *Gertisser and Keller* [2000]; *Peccerillo* [2005]; *Lucchi et al.* [2013d]. Stromboli, *Ellam et al.* [1989]; *Francalanci et al.* [1989, 1993, 1999, 2004, 2008, 2012, 2013]; *De Astis et al.* [2000]; *Landi et al.* [2006, 2009]; *Tommasini et al.* [2007]; *Corazzato et al.* [2008]; *Petrone et al.* [2009].

Kawamoto et al. [2012] demonstrated that a supercritical fluid derived from the slab could separate to form fluid and melt components in most subduction zones. We can use trace elements that are compatible in either hydrous fluids or melts to discriminate between these two subduction components. For instance, the high field strength elements (HFSE, e.g., Nb, Ta, Zr, Th) and middle to heavy rare earth elements (REE) preferentially partition into melts. The alkali metals (e.g., K, Rb), the alkaline earth metals (e.g., Ba, Sr), and U are soluble-lithophile elements because hydrous fluids preferentially mobilize these elements. Similarly, light REE (e.g., La) are mobilized more easily by hydrous fluid than the rest of the REE [*Brenan et al.*, 1995; *Johnson and Plank*, 1999; *Elliott*, 2003; *Turner et al.*, 2003].

Once elemental behaviors are understood, then element ratios can be used to minimize the effect of partial melting and fractionation processes on the determination of geochemical signatures. For example, commonly used ratios of elements mobilized by subduction related fluids to those mobilized only in melts (e.g., Ba/Nb, U/Th, Sr/La) are highest in the central segment of the Aeolian Arc (Salina), while for the external islands (particularly Stromboli) these ratios are low, consistent with the increased contribution of silicate melt components (Figure 5). These along-arc variations suggest that fluids play a major role in element transport into the mantle wedge beneath the central region of the arc (Salina), while under Stromboli and, to a lesser extent under Alicudi, a silicate melt is the dominant contributing component. Based on isotopic evidence, *Tonarini et al.* [2001] also suggested the important role of a hydrous fluid component in the magma genesis in the central sector of the Aeolian arc.

In this study, we also explore these element systematics further by the use of additional fluid mobile elements (e.g., B, As, Li), and Be, a melt-soluble element, as geochemical indicators of subduction components (Figure 3) [*Leeman*, 1996; *Ryan et al.*, 1996a] with the goal to better discriminate between slab-derived fluid and melt signatures in the Aeolian Arc. While B and As mobilize in slab fluids starting very early in the subduction process, Li is largely retained on the slab until temperatures increase, and it is also retained in the mantle wedge much better than B or As, because it can substitute for Mg [*Bebout et al.*, 1999; *Bebout*, 2007; *Savov et al.*, 2005, 2007; *Penniston-Dorland et al.*, 2012]. In the subducting slab, B and Be are most likely going to be hosted by phengitic white micas while Li will be host by phengite and chlorite. Due to B high mobility in fluids while at the same time, Be is going to be strongly retained in phengite and only mobilized by melts [e.g., *Bebout et al.*, 1999], their relative concentrations in resulting arc magmas are considered to be powerful indicators of the role of fluids versus melt components in subduction zones. Arsenic behaves in slab metasediments very much like B [e.g. *Noll et al.*, 1996], so we can infer that its phengite-fluid partitioning behavior is similar to B. Additionally, neither B nor Be are going to be impacted by accessory phases like tourmaline and beryl as usually these phases can be stable under extreme high silica concentrations [e.g., *London and Evensen*, 2002; *Marschall et al.*, 2009]. Tourmaline in ultrahigh-pressure metamorphic rocks requires silica-rich fluids; however, it is also a common trace phase in medium to high-grade metasediments [*Marschall et al.*, 2009]. Arsenic concentrations can be strongly controlled by segregating sulfide phases, but

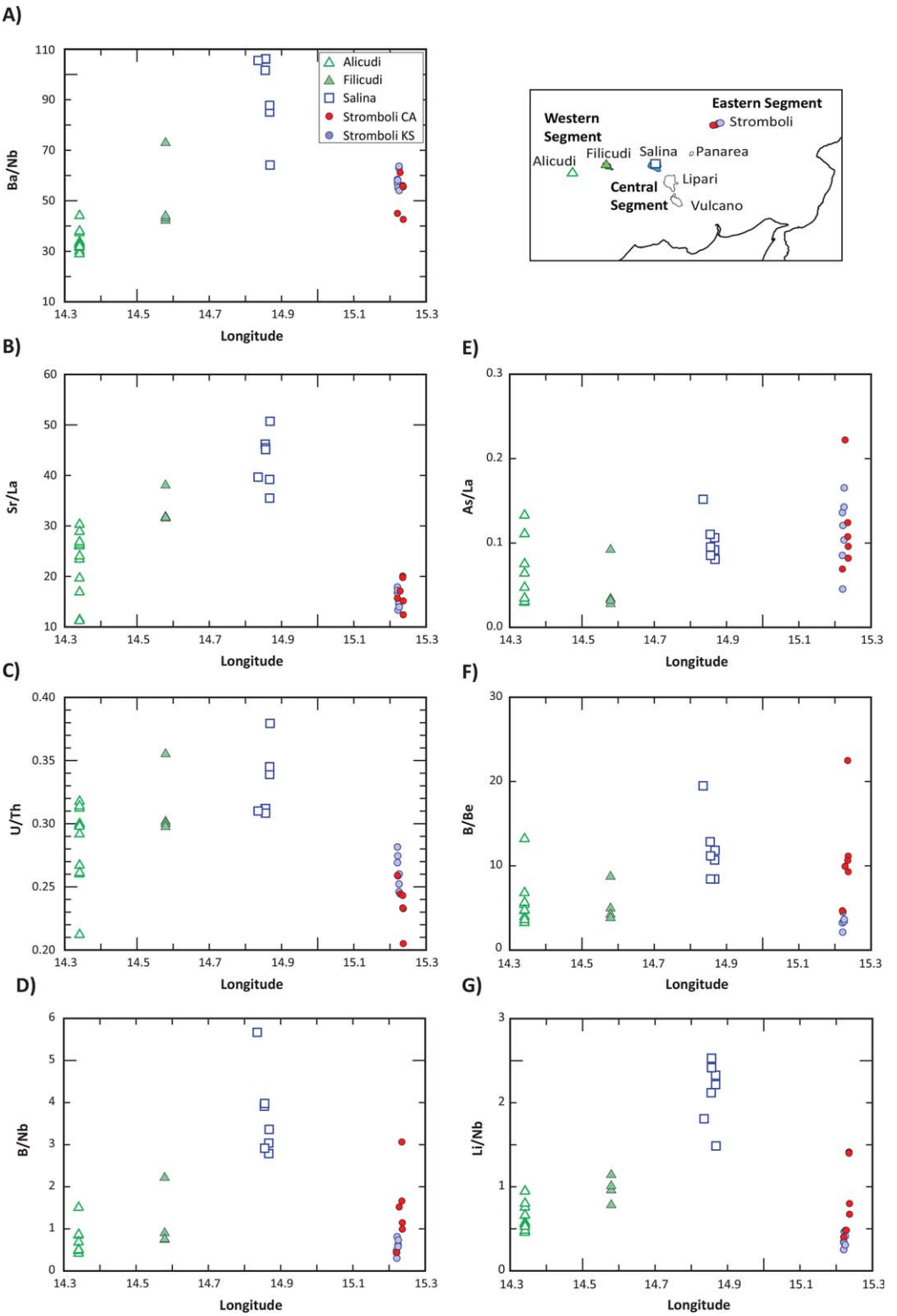

Figure 5. Regional along-arc variations of elements mobilized by hydrous fluids (e.g., Ba, Sr, U, B, As, Li) over elements soluble in melts (e.g., Nb, Th, Be) for the Aeolian samples of this study. Note how the central segment of the arc has higher fluid/melt ratios while the peripheral arc segments are controlled by melt soluble elements.

the oxidized nature of volcanic arc melts generally suppresses sulfide during fractional crystallization [*Hattori et al*., 2002].

Boron is particularly useful as it is strongly enriched in marine sediments and altered oceanic crust, and is extremely depleted in the upper mantle [*Leeman and Sisson*, 1996; *Bebout et al*., 1999; *Plank*, 2014; *Ryan and Chauvel*, 2014]. The general increase in B contents toward the eastern segment of the Aeolian Arc (Figure 3a) is best explained by hydrous fluid inputs derived from the dehydrating subducting slab and sediments, as also evident by other trace element systematics (Figures 5a–5c). Boron enrichment can be evaluated also in details with B/Nb and B/Be ratios (Figures 5d and 5f), because these ratios reflect the extent of influence of fluid-related process more than varying extents of partial melting and fractional crystallization. B/Nb and B/Be increase from west to east reaching a peak in Salina and then drop off in Stromboli. This "chevron pattern" indicates that the degree of enrichment of boron is higher in Salina and lower at the peripheral islands regardless of the element concentration that can be controlled by degree of melting of fractional crystallization. A very similar trend is also observed for the other fluid mobile elements (e.g., Li/Nb, Figure 5g) along the volcanic front; nevertheless, As (e.g., As/La, Figure 5e) shows a slightly increase from west to east and it might be indicative of subducting sulfidic or hydroxide-rich sediments.

Typically B and other fluid-mobile elements (e.g., As, Sb) are also highly enriched in serpentinite, which is a very important component in a shallow mantle wedge due to its strong enrichment in water. Dehydration of serpentine plays an important role in triggering melt in subarc mantle depths [*Scambelluri and Tonarini*, 2012]. Although the extent of mobilization of these elements via low-temperature hydrous fluid can be considerable (as much as 70% of the slab budget for B and $>$15% for As) [*Savov et al*., 2005, 2007], a serpentinite component is probably not involved in the genesis of the Aeolian Arc magmas. This consideration can be deduced by the B isotopic data presented by *Tonarini et al*. [2001], in which the value of δ^{11}B are too low (-6.1 to $+2.3‰$) to be derived from a serpentinite source, in contrast to the high B isotopic values (up to $+18‰$) that would be characteristic of a serpentinite-derived fluid [e.g., *Benton et al*., 2001], and the generally elevated δ^{11}B signatures ($>+5‰$, for details see the study review of *Ryan and Chauvel*, 2014] of B-enriched arcs such as South Sandwich [*Tonarini et al*., 2011], the Izu-Bonin-Mariana [*Ishikawa and Nakamura*, 1994; *Ishikawa and Tera*, 1999; *Straub and Layne*, 2002], and the Kuril-Kamchatka [*Ishikawa and Tera*, 1997; *Ishikawa et al*., 2001]. The global compilation of volcanic arc B and δ^{11}B data in *Ryan and Chauvel* [2014] demonstrates a dichotomy in subduction systems, correlated to their overall thermal structures, in which most show evidence for the involvement of a high B, high δ^{11}B component, consistent with serpentinite-derived fluids, with a few "hot" systems (e.g., Cascades, Mexico) in which this component appears to play no role, due perhaps to the release of B early enough during subduction that it is not carried to mantle depths (see additional discussion in section 4.1).

Beryllium is typically concentrated in marine sediments, and is very depleted in the upper mantle, mimicking the terrestrial distribution pattern of boron [*Morris et al*., 1990; *Ryan*, 2002; *Plank*, 2014; *Ryan and Chauvel*, 2014]. Although Be is also a light element, it is very different from boron in terms of behavior, in that it is immobile in hydrous fluids but highly mobile in silicate melts derived from a subducting slab [*Brenan et al*., 1998; *Ryan*, 2002]. Although, the beryllium contents in calc-alkaline lavas from across the Aeolian Arc are largely similar (Figure 3b), it is strongly enriched in the potassic samples from Stromboli (Figure 3b), as are other incompatible trace elements. This behavior can be explained by partial melting of a source that is broadly enriched in incompatible trace elements, including Be. Thus, we suggest that this source is consistent with subducted sediments transported into the mantle wedge by the Ionian slab. The role of silicate melts in Stromboli is also evident when Be contents of different islands are plotted against B in respect to Upper Mantle (UM) values (Figure 3e). Due to the different compositional trends displayed in Figure 3e, we suggest two different sources for the calc-alkaline and potassic rocks of Stromboli (in agreement with other geochemical tracers used by *Tommasini et al*. [2007] and *Francalanci et al*. [2013]), a fluid component derived from the oceanic slab for the calc-alkaline magmas and a sediment melt component for the potassic rocks. The potassic lavas of Stromboli show high Th/Ce and low ^{143}Nd/^{144}Nd as compared to the other islands of the Aeolian Arc [*Francalanci et al*., 2007], a clear signature that can be obtained by a sediment melt component [*Elliott et al*., 1997; *Hawkesworth et al*., 1997; *Johnson and Plank*, 1999; *Class et al*., 2000]. These results are also consistent with B and Be data collected for young Vesuvius lavas by *Morris et al*. [1993], that also suggest a sediment melt-dominated component.

Similarities in the trends of other fluid mobile elements (e.g., As and Li) relative to B versus Be (Figures 3f and 3g) provide additional evidence for a clear separation between the two magmatic end-members in this

arc. Figure 5d shows that values in B/Nb, with a peak found at Salina, are similar to the ratios reported by *Ryan et al*. [1996b], in which the partition coefficients of B and Nb are very similar ($D_B \sim D_{Nb}$). Also, the fact that the Li/Nb and K/La both show patterns similar to those of the B/Nb and B/La suggests that the slab component being sampled in this area is enriched in alkali elements. Furthermore, the Be/Nd ratio for Alicudi, Filicudi and Salina rocks varies slightly from the global arc ratio (∼0.05) [*Ryan and Langmuir*, 1988], while Stromboli basalts are characterized by higher ratios relative to typical arc magmas that may relate to a slab component enriched in alkaline elements.

In order to explain the higher values for Be and Nb in the potassic lavas from Stromboli (supporting information Table S1C and S1D), the sediment-melt component must be dominant in the genesis of these lavas. Experimental work suggested that silica-undersaturated alkaline arc lavas could be produced via the reaction of sediment-derived siliceous melt with peridotite in the mantle wedge [*Avanzinelli et al*., 2008; *Mallik and Dasgupta*, 2013]. More recently, an experimental study by *Mallik et al*. [2015] demonstrated that ultrapotassic magmas (resembling the ones from Stromboli) can be generated by mantle reaction with hydrous sediment-derived melts. *Mallik et al*. [2015] indicated that during reactions between hydrous sediment-derived partial melts of rhyolitic composition and peridotite, the stabilization of orthopyroxene and phlogopite reduces the silica content of the melt, and buffers the composition toward higher K_2O contents, yielding compositions resembling the ultrapotassic lavas from the Sunda Arc and from the Roman Magmatic Province.

4.1. Contrasting the Aeolian Arc With Other Global Volcanic Arc Examples

Understanding how these new data fit into global systematics of volcanic arcs is key for the interpretation of the geodynamic complexity of the Aeolian Arc. We have compared our new B, Be, and trace-element data with samples from the Phlegrean Fields, along with other well studied volcanic arcs and arc segments in the world by assembling a data set via the GEOROC database (http://georoc.mpch-mainz. gwdg.de/georoc/) accessed in February 2015.

Boron enrichments in Aeolian Arc lavas are consistently low, with B/Be ratios ranging between ∼2 and 15 in most samples (Figure 5f). This makes the Aeolian Arc comparable to the Cascades and the Mexican Volcanic Belt (∼2–12 and ∼1–15, respectively) arcs as "low boron" subduction systems, a trait that is also evident in its B-isotopic systematics [e.g., *Tonarini et al*., 2001]. These similarities are clear in Figure 6a, a plot of Th/Nb versus La/Nb, in which mixing between potential end-members will form linear arrays. This plot allows us to distinguish between melt components (high Th/Nb and low La/Nb) and fluid components (low Th/Nb and high La/Nb) as slab-derived metasomatizing agents in the different arcs. In this diagram, the Stromboli data overlap with data for the Sunda Arc, the Phlegrean Fields, and partially with the Cascades data along a trend controlled by a melt-dominated component, clearly separating from the other Aeolian Islands, which display increasing La/Nb, from west to east. Alicudi, Filicudi, and Salina overlap the data field for the Aleutian Arc, and part of the Marianas, Kamchatka, and the Mexican Volcanic Belt, indicating a transitional nature between the melt and fluid trends. Meanwhile, the fluid component dominates in the Izu-Bonin, Marianas, Kamchatka, and Tonga Arcs. Comparable behaviors can also be inferred from a plot of Th/Nb versus Ba/Nb (Figure 6b).

Figure 6c plots B/Nb versus Th/Nd to further discriminate between fluid and melt components. B/Nb is a tracer of slab fluid released by dehydration of sediment and altered oceanic crust [*Ishikawa and Tera*, 1997] while Th/Nd is a tracer of sediment melt in arc magmas [*Class et al*., 2000]. The curved line represents a potential mixing between a fluid-controlled end-member (represented by Izu Bonin samples), and a melt-dominated end-member (represented by the Sunda Arc, Phlegrean Fields, and Stromboli). The fact that most of the arc samples included in this comparison plot between these end-members suggests that likely in all arcs worldwide slab-derived fluids and melts are responsible in different proportions for the subduction-related elemental enrichments seen in arc lavas. The dominant component will depend on the thermal structure of the arc, as is evident in arc B/La versus Ba/La systematics (Figure 6d) [see *Ryan and Chauvel*, 2014]. The Aeolian suite forms a trend at low B/La consistent with the mixing of a "hot" slab-derived B source and the upper mantle [*Ryan and Chauvel*, 2014]. The fluid-mobile element systematics of Aeolian lavas are thus different from those volcanic arcs such as Izu-Bonin, Marianas, Kamchatka, and Central America (Honduras-Nicaragua) as there is no evidence for the involvement of a "cool" slab-derived B source, suggested to involve contributions from subduction-related serpentinite [e.g., *Straub and Layne*,

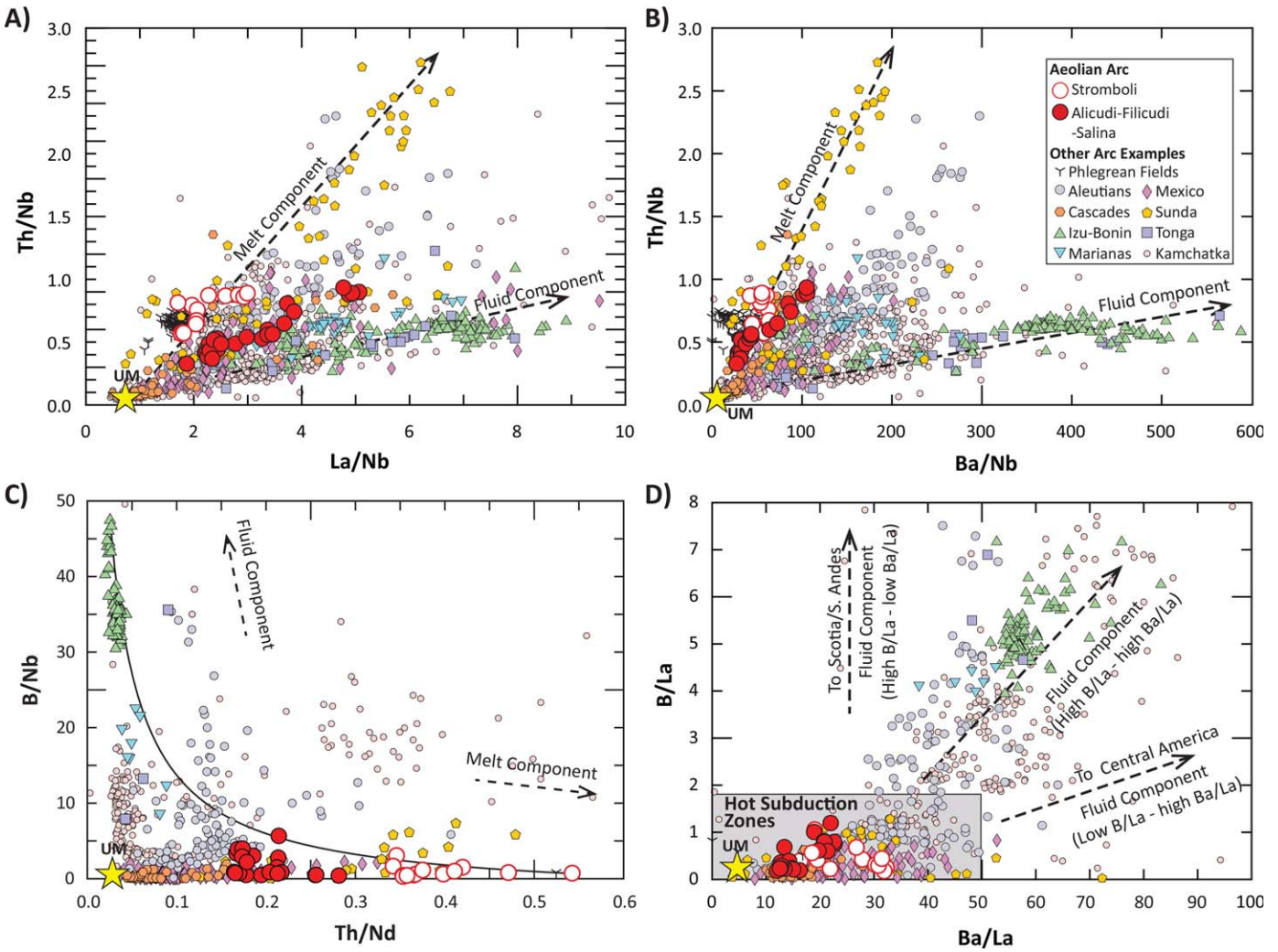

Figure 6. Element ratios discriminating between slab-derived fluid components versus melt components. Different elements ratios (Th/Nb, La/Nb, Ba/Nb, B/Nb, and Th/Nd) are used to discriminate between sediment melts and slab-fluid components for volcanic arcs/arc segments (a, b, c). In Figure 6c, the curve represents a binary mixing between a fluid (Izu-Bonin) and melt (Stromboli, Phlegrean Fields, and Sunda) end-member. In Figure 6d, low values of B/La and Ba/La define the "hot subduction zones" where fluid mobile elements get removed early during subduction processes as described by *Ryan and Chauvel* [2014]. Global data for the Phlegrean Fields, Aleutians, Kamchatka, Izu-Bonin, Tonga, Sunda, Marianas, Mexican Volcanic Belt, and Cascades are from the GEOROC geochemical database (http://georoc.mpch-mainz.gwdg.de/georoc/). Upper Mantle (UM) derived melts are from the same reference sources as in Figure 3.

2002; *Savov et al*., 2005, 2007; *Hattori and Guillot*, 2007; *Tonarini et al*., 2007; *Ryan and Chauvel*, 2014]. While the "cool" fluid-mobile element component is not evident in Aeolian lavas, the fact that they nonetheless show boron enrichment indicates that a slab-derived fluid component is involved.

4.2. Geodynamic Implications

Global thermal models for subduction systems from *Syracuse et al*. [2010] describe different pressure-temperature (P-T) paths of subducting slabs using kinematically defined slabs based on physical parameters (e.g., slab geometries, ages, convergence velocities). The model (D80) portrays the subduction of the Ionian slab beneath Calabria as one of the coldest subduction zones on Earth (Figure 7). This observation is not consistent with the observed geochemical signatures, which suggest a substantial sediment melt component, as the slab P-T path will not even cross the water-saturated sediment solidus (Figure 7). Nevertheless, the *Syracuse et al*. [2010] results come from a two-dimensional model that does not consider the 3-D complications of lateral or trench-parallel asthenospheric mantle flow, due to slab rollback or slab windows, [*Buttles and Olson*, 1998; *Stegman et al*., 2006; *Schellart*, 2008], a process that may exist in many subduction systems. For example, the mantle wedge below the Sunda Arc is affected by flow of upwelling asthenosphere through a horizontal slab window [*Richards et al*., 2007; *Whittaker et al*., 2007; *Kundu and*

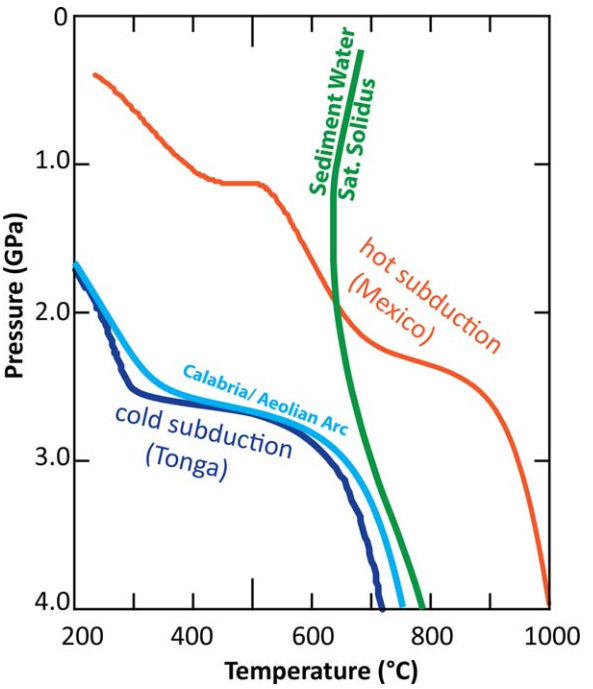

Figure 7. Pressure-temperature diagram for the Aeolian Arc (Calabria) subducting slab (model D80, from *Syracuse et al.* [2010]) compared to a cold subduction zone end-member (Tonga) and a hot subducting zone end-member (Mexico). Note that according to the numerical models the Ionian slab does not intersect the water saturated-sediment solidus [from *Mann and Schmidt*, 2015]. Thus, in order to have sediment melt signatures, we need another process that will either increase the temperature of the slab or cause the separation of sediment diapirs that will cross the solidus before the slab gets dehydrated.

Gahalaut, 2011] but aging in the Syracuse's model this arc is not pictured especially hot as suggested by the geochemical data. The geochemical variations in the northern segment of the Cascades are in fact best explained by asthenosphere toroidal flow from the northern edge of Juan de Fuca subducting plate [*Mullen and Weis*, 2015]. Also, the origin of the heterogeneous mantle under the Mexican Volcanic Belt and Southern Central America are also explained by influx of hotter asthenosphere along a trench-parallel slab window in the Cocos Plate at the edges of the subducting slab [*Ferrari*, 2004; *Gazel et al.*, 2011; *Ferrari et al.*, 2012].

Seismic studies and numerical models in the southern Tyrrhenian area [*Chiarabba et al.*, 2008; *Baccheschi et al.*, 2008, 2011; *Neri et al.*, 2012; *Faccenna et al.*, 2011] suggest the presence of African-related asthenospheric flow around the edges of the narrow Ionian Plate due to a slab tear caused by the rollback motion of the Ionian slab [*Gvirtzman and Nur*, 1999], which heavily affected the mantle wedge of the Aeolian Arc [e.g., *Faccenna et al.*, 2011]. Also, recent work by *Chen et al.* [2015] based on dynamic laboratory models of progressive subduction in three-

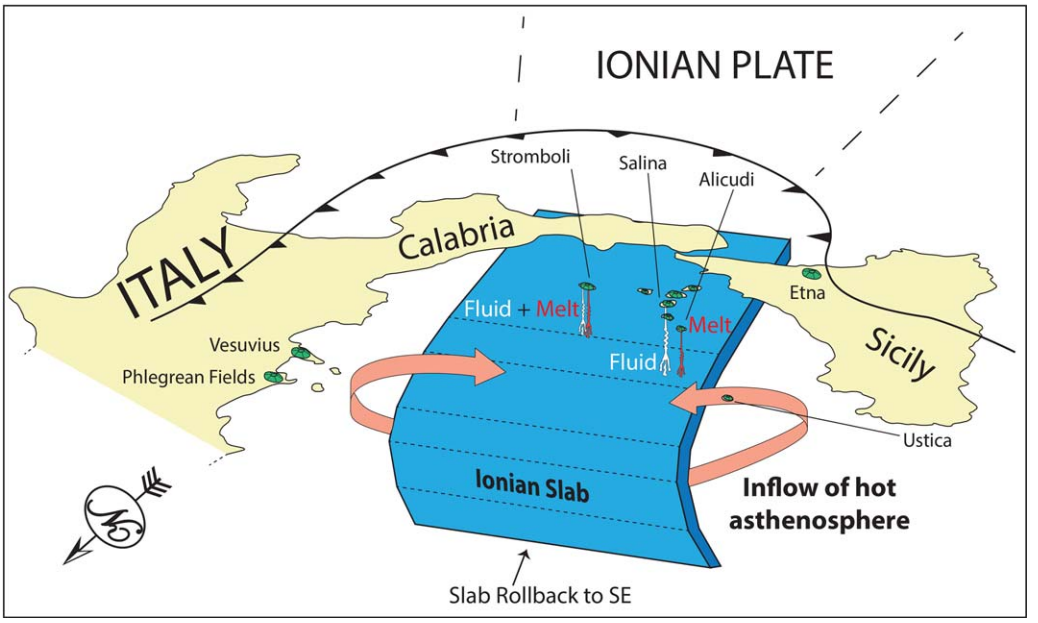

Figure 8. Schematic model representing the Ionian slab subduction system below the Aeolian Arc modified from *Trua et al.* [2007]. Orange arrows indicate the asthenospheric mantle inflow over the edges of the Ionian Plate rollbacking toward the SE. The predominant melt components are represented in red under Stromboli and Alicudi. The predominant fluid component is represented in white under Stromboli and Salina.

dimensional space highlights the possibility of a toroidal asthenosphere return flow induced by the slab rollback of the Ionian Plate. Our new data confirm a sediment melt component at the borders of the arc, possibly connected to hot asthenosphere flow at the edges of the slab responsible for the melt signature (Figure 8). Alternatively, buoyant diapirs of slab material can potentially detach from the subducting slab and enter a regime of elevated temperatures in the mantle wedge that will cause devolatilization and melting of such rocks and the delivery of the different slab component signatures [*Hacker et al*., 2011; *Marschall and Schumacher*, 2012]. Nevertheless this model still does not explain the systematic variations in the different arc segments of the Aeolian arc (one section of the arc is controlled by hydrous fluids and another is controlled by both slab melts and fluids components) that are still point toward the possibility of hot asthenosphere flow at the edge of the subducting slab.

5. Concluding Remarks

The Aeolian Arc exhibits strong along-arc geochemical variations. Based on the systematics of B, Be, Li, and As contents in the Aeolian lavas, we infer that fluids from the subducting altered oceanic lithosphere influence the whole arc, in particular the central sector. We confirmed the presence of a slab melt component at the peripheral islands, especially evident in the potassic lavas in Stromboli, that display some of the highest Be contents reported in arc global lavas.

We propose that the melt component is represented by a partial melt of sediments transported by the subducting Ionian slab. Hot asthenosphere inflow around the borders of the subducting Ionian Plate could potentially explain the presence of this component. This process explains why the Aeolian Arc shares clear geochemical similarities to hot subduction zones like the Cascades and the Mexican Volcanic Belt, rather than the expected cold conditions from numerical models.

Acknowledgments
Geographic locations, sample description and new geochemical data are included in the supporting information Data Set S1. Revisions and comments by an anonymous reviewer and Sarah Penniston-Dorland improved the original manuscript. This project benefited from discussion with Terry Plank, Paul Wallace, Jim Gill, and Peter van Keken. Finally, we appreciate the editorial handling of Cin-Ty Lee and analytical support by Luca Fedele.

References

Avanzinelli, R., T. Elliott, S. Tommasini, and S. Conticelli (2008), Constraints on the genesis of potassium-rich Italian volcanic rocks from U/Th disequilibrium, *J. Petrol.*, *49*(2), 195–223, doi:10.1093/petrology/egm076.

Avanzinelli, R., J. Prytulak, S. Skora, A. Heumann, G. Koetsier, and T. Elliott (2012), Combined 238U–230Th and 235U–231Pa constraints on the transport of slab-derived material beneath the Mariana Islands, *Geochim. Cosmochim. Acta*, *92*, 308–328, doi:10.1016/j.gca.2012.06.020.

Baccheschi, P., L. Margheriti, and M. S. Steckler (2008), SKS splitting in Southern Italy: Anisotropy variations in a fragmented subduction zone, *Tectonophysics*, *462*(1–4), 49–67, doi:10.1016/j.tecto.2007.10.014.

Baccheschi, P., L. Margheriti, M. S. Steckler, and E. Boschi (2011), Anisotropy patterns in the subducting lithosphere and in the mantle wedge: A case study—The southern Italy subduction system, *J. Geophys. Res.*, *116*, B08306, doi:10.1029/2010JB007961.

Barry, T. L., J. A. Pearce, P. T. Leat, I. L. Millar, and A. P. le Roex (2006), Hf isotope evidence for selective mobility of high-field-strength elements in a subduction setting: South Sandwich Islands, *Earth Planet. Sci. Lett.*, *252*(3–4), 223–244, doi:10.1016/j.epsl.2006.09.034.

Bebout, G. E. (2007), Metamorphic chemical geodynamics of subduction zones, *Earth Planet. Sci. Lett.*, *260*(3–4), 373–393, doi:10.1016/j.epsl.2007.05.050.

Bebout, G. E., J. G. Ryan, W. P. Leeman, and A. E. Bebout (1999), Fractionation of trace elements by subduction-zone metamorphism—effect of convergent-margin thermal evolution, *Earth Planet. Sci. Lett.*, *171*(1), 63–81.

Beccaluva, L., P. L. Rossi, and G. Serri (1982), Neogene to Recent volcanism of the southern Tyrrhenian-Sicilian area: Implications for the geodynamic evolution of the Calabrian arc, *Earth Evol. Sci.*, *3*, 222–238.

Beccaluva, L., G. Gabbianelli, F. Lucchini, P. L. Rossi, and C. Savelli (1985), Petrology and K/Ar ages of volcanics dredged from the Eolian seamounts: Implications for geodynamic evolution of the southern Tyrrhenian basin, *Earth Planet. Sci. Lett.*, *74*(2), 187–208.

Beccaluva, L., et al. (1990), Geochemistry and mineralogy of volcanic rocks from ODP sites 650, 651, 655 and 654 in the Tyrrhenian Sea, *Proc. Ocean Drill. Program Sci. Results*, *107*, 49–74.

Benton, L. D., J. G. Ryan, and F. Tera (2001), Boron isotope systematics of slab fluids as inferred from a serpentine seamount, Mariana forearc, *Earth Planet. Sci. Lett.*, *187*(3–4), 273–282, doi:10.1016/S0012-821X(01)00286-2.

Brenan, J. M., H. F. Shaw, and F. J. Ryerson (1995), Experimental evidence for the origin of lead enrichment in convergent-margin magmas, *Nature*, *378*, 54–56.

Brenan, J. M., F. J. Ryerson, and H. F. Shaw (1998), The role of aqueous fluids in the slab-to-mantle transfer of boron, beryllium, and lithium during subduction: Experiments and models, *Geochim. Cosmochim. Acta*, *62*(19), 3337–3347.

Buttles, J., and P. Olson (1998), A laboratory model of subduction zone anisotropy, *Earth Planet. Sci. Lett.*, *164*(1), 245–262.

Chen, Z., W. P. Schellart, and J. C. Duarte (2015), Overriding plate deformation and variability of fore-arc deformation during subduction: Insight from geodynamic models and application to the Calabria subduction zone, *Geochem. Geophys. Geosyst.*, *16*, 3697–3715, doi:10.1002/2015GC005958.

Chiarabba, C., P. De Gori, and F. Speranza (2008), The southern Tyrrhenian subduction zone: Deep geometry, magmatism and Plio-Pleistocene evolution, *Earth Planet. Sci. Lett.*, *268*(3–4), 408–423, doi:10.1016/j.epsl.2008.01.036.

Class, C., D. M. Miller, S. L. Goldstein, and C. H. Langmuir (2000), Distinguishing melt and fluid subduction components in Umnak Volcanics, Aleutian Arc, *Geochem. Geophys. Geosyst.*, *1*(6), 1004, doi:10.1029/1999GC000010.

Corazzato, C., L. Francalanci, M. Menna, C. M. Petrone, A. Renzulli, A. Tibaldi, and L. Vezzoli (2008), What controls sheet intrusion in volcanoes? Structure and petrology of the Stromboli sheet complex, Italy, *J. Volcanol. Geotherm. Res.*, *173*(1–2), 26–54, doi:10.1016/j.jvolgeores.2008.01.006.

De Astis, G., G. Ventura, and G. Vilardo (2003), Geodynamic significance of the Aeolian volcanism (Southern Tyrrhenian Sea, Italy) in light of structural, seismological, and geochemical data, *Tectonics*, *22*(4), 1040, doi:10.1029/2003TC001506.

De Astis, G., A. Peccerillo, P. D. Kempton, L. La Volpe, and T. W. Wu (2000), Transition from calc-alkaline to potassium-rich magmatism in subduction environments: Geochemical and Sr, Nd, Pb isotopic constraints from the island of Vulcano (Aeolian arc), *Contrib. Mineral. Petrol.*, *139*(6), 684–703.

De Astis, G., P. D. Kempton, A. Peccerillo, and T. W. Wu (2006), Trace element and isotopic variations from Mt. Vulture to Campanian volcanoes: Constraints for slab detachment and mantle inflow beneath southern Italy, *Contrib. Mineral. Petrol.*, *151*(3), 331–351, doi:10.1007/s00410-006-0062-y.

De Astis, G., F. Lucchi, P. Dellino, L. La Volpe, C. A. Tranne, M. L. Frezzotti, and A. Peccerillo (2013), Geology, volcanic history and petrology of Vulcano (central Aeolian archipelago), *Geol. Soc. London Mem.*, *37*(1), 281–349, doi:10.1144/M37.

Di Martino, C., M. L. Frezzotti, F. Lucchi, A. Peccerillo, C. A. Tranne, and L. W. Diamond (2010), Magma storage and ascent at Lipari Island (Aeolian archipelago, Southern Italy) at 223–81 ka: The role of crustal processes and tectonic influence, *Bull. Volcanol.*, *72*(9), 1061–1076, doi:10.1007/s00445-010-0383-6.

Di Martino, C., F. Forni, M. L. Frezzotti, R. Palmeri, J. D. Webster, R. A. Ayuso, F. Lucchi, and C. A. Tranne (2011), Formation of cordierite-bearing lavas during anatexis in the lower crust beneath Lipari Island (Aeolian arc, Italy), *Contrib. Mineral. Petrol.*, *162*(5), 1011–1030, doi:10.1007/s00410-011-0637-0.

Eiler, J. M., M. J. Carr, M. Reagan, and E. Stolper (2005), Oxygen isotope constraints on the sources of Central American arc lavas, *Geochem. Geophys. Geosyst.*, *6*, Q07007, doi:10.1029/2004GC000804.

Ellam, R. M. (1986), *The transition of calc-alkaline to potassic volcanism in the Aeolian Islands, southern Italy*, Ph.D thesis, Open Univ., Milton, Keynes, U. K.

Ellam, R. M., and R. S. Harmon (1990), Oxygen isotope constraints on the crustal contribution to the subduction-related magmatism of the Aeolian Islands, southern Italy, *J. Volcanol. Geotherm. Res.*, *44*(1), 105–122.

Ellam, R. M., M. A. Menzies, C. J. Hawkesworth, W. P. Leeman, M. Rosi, and G. Serri (1988), The transition from calc-alkaline to potassic orogenic magmatism in the Aeolian Islands, Southern Italy, *Bull. Volcanol.*, *50*(6), 386–398.

Ellam, R. M., C. J. Hawkesworth, M. A. Menzies, and N. W. Rogers (1989), The volcanism of southern Italy: Role of subduction and the relationship between potassic and sodic alkaline magmatism, *J. Geophys. Res.*, *94*(B4), 4589–4601, doi:10.1029/JB094iB04p04589.

Elliott, T. (2003), Tracers of the slab, in *Inside the Subduction Factory, Geophys. Monogr. Ser.*, vol. 138, edited by J. Eiler, pp. 23–45, AGU, Washington, D. C., doi:10.1029/138GM03.

Elliott, T., T. Plank, A. Zindler, W. White, and B. Bourdon (1997), Element transport from slab to volcanic front at the Mariana arc, *J. Geophys. Res.*, *102*(B7), 14,991–15,019, doi:10.1029/97JB00788.

Faccenna, C., P. Molin, B. Orecchio, V. Olivetti, O. Bellier, F. Funiciello, L. Minelli, C. Piromallo, and A. Billi (2011), Topography of the Calabria subduction zone (southern Italy): Clues for the origin of Mt. Etna, *Tectonics*, *30*, TC1003, doi:10.1029/2010TC002694.

Falsaperla, S., G. Lanzafame, V. Longo, and S. Spampinato (1999), Regional stress field in the area of Stromboli (Italy): Insights into structural data and crustal tectonic earthquakes, *J. Volcanol. Geotherm. Res.*, *88*(3), 147–166.

Ferrari, L. (2004), Slab detachment control on mafic volcanic pulse and mantle heterogeneity in central Mexico, *Geology*, *32*(1), 77, doi:10.1130/G19887.1.

Ferrari, L., T. Orozco-Esquivel, V. Manea, and M. Manea (2012), The dynamic history of the Trans-Mexican Volcanic Belt and the Mexico subduction zone, *Tectonophysics*, *522–523*, 122–149, doi:10.1016/j.tecto.2011.09.018.

Foley, S. F., M. G. Barth, and G. A. Jenner (2000), Rutile/melt partition coefficients for trace elements and an assessment of the influence of rutile on the trace element characteristics of subduction zone magmas, *Geochim. Cosmochim. Acta*, *64*(5), 933–938, doi:10.1016/S0016-7037(99)00355-5.

Forni, F., F. Lucchi, A. Peccerillo, C. A. Tranne, P. L. Rossi, and M. L. Frezzotti (2013), Stratigraphy and geological evolution of the Lipari volcanic complex (central Aeolian archipelago), *Geol. Soc. London Mem.*, *37*(1), 213–279, doi:10.1144/M37.10.

Francalanci, L., and A. P. Santo (1993), Magmatological evolution of Filicudi volcanoes, Aeolian Islands, Italy: Constraints from mineralogical, geochemical and isotopic data, *Acta Vulcanol.*, *3*, 203–227.

Francalanci, L., P. Manetti, and A. Peccerillo (1989), Volcanological and magmatological evolution of Stromboli volcano (Aeolian Islands): The roles of fractional crystallization, magma mixing, crustal contamination and source heterogeneity, *Bull. Volcanol.*, *51*(5), 355–378.

Francalanci, L., S. R. Taylor, M. T. McCulloch, and J. D. Woodhead (1993), Geochemical and isotopic variations in the calc-alkaline rocks of Aeolian arc, southern Tyrrhenian Sea, Italy: Constraints on magma genesis, *Contrib. Mineral. Petrol.*, *113*(3), 300–313.

Francalanci, L., S. Tommasini, S. Conticelli, and G. R. Davies (1999), Sr isotope evidence for short magma residence time for the 20th century activity at Stromboli volcano, Italy, *Earth Planet. Sci. Lett.*, *167*(1), 61–69.

Francalanci, L., S. Tommasini, and S. Conticelli (2004), The volcanic activity of Stromboli in the 1906–1998 AD period: Mineralogical, geochemical and isotope data relevant to the understanding of the plumbing system, *J. Volcanol. Geotherm. Res.*, *131*(1–2), 179–211, doi:10.1016/s0377-0273(03)00362-7.

Francalanci, L., R. Avanzinelli, S. Tommasini, and A. Heuman (2007), A west-east geochemical and isotopic traverse along the volcanism of the Aeolian Island arc, southern Tyrrhenian Sea, Italy: Inferences on mantle source processes, *Geol. Soc. Am. Spec. Pap.*, *418*, 235–263, doi:10.1130/2007.2418(12).

Francalanci, L., A. Bertagnini, N. Métrich, A. Renzulli, R. Vannucci, P. Landi, S. Del Moro, M. Menna, C. M. Petrone, and I. Nardini (2008), Mineralogical, geochemical, and isotopic characteristics of the ejecta from the 5 April 2003 paroxysm at Stromboli, Italy: Inferences on the preeruptive magma dynamics, in *The Stromboli Volcano: An Integrated Study of the 2002-2003 Eruption, Geophys. Monogr. Ser.*, vol. 183, edited S. Calvari et al., pp. 331–345, AGU, Washington, D. C.

Francalanci, L., R. Avanzinelli, I. Nardini, M. Tiepolo, J. P. Davidson, and R. Vannucci (2012), Crystal recycling in the steady-state system of the active Stromboli volcano: A 2.5-ka story inferred from in situ Sr-isotope and trace element data, *Contrib. Mineral. Petrol.*, *163*(1), 109–131, doi:10.1007/s00410-011-0661-0.

Francalanci, L., F. Lucchi, J. Keller, G. De Astis, and C. A. Tranne (2013), Eruptive, volcano-tectonic and magmatic history of the Stromboli volcano (north-eastern Aeolian archipelago), *Geol. Soc. London, Mem.*, *37*(1), 397–471, doi:10.1144/M37.13.

Gale, A., C. A. Dalton, C. H. Langmuir, Y. Su, and J.-G. Schilling (2013), The mean composition of ocean ridge basalts, *Geochem. Geophys. Geosyst.*, *14*, 489–518, doi:10.1029/2012GC004334.

Gazel, E., M. J. Carr, K. Hoernle, M. D. Feigenson, D. Szymanski, F. Hauff, and P. van den Bogaard (2009), Galapagos-OIB signature in southern Central America: Mantle refertilization by arc-hot spot interaction, *Geochem. Geophys. Geosyst.*, *10*, Q02S11, doi:10.1029/2008GC002246.

Gazel, E., K. Hoernle, M. J. Carr, C. Herzberg, I. Saginor, P. v. den Bogaard, F. Hauff, M. Feigenson, and C. Swisher (2011), Plume–subduction interaction in southern Central America: Mantle upwelling and slab melting, *Lithos*, *121*(1–4), 117–134, doi:10.1016/j.lithos.2010.10.008.

Gazel, E., et al. (2015), Continental crust generated in oceanic arcs, *Nat. Geosci.*, *8*(4), 321–327, doi:10.1038/ngeo2392.

Gertisser, R., and J. Keller (2000), From basalt to dacite: Origin and evolution of the calc-alkaline series of Salina, Aeolian Arc, Italy, *Contrib. Mineral. Petrol.*, *139*(5), 607–626.

Gill, J. B. (1981), *Orogenic Andesites and Plate Tectonics*, Springer, N. Y.

Gvirtzman, Z., and A. Nur (1999), The formation of Mount Etna as the consequence of slab rollback, *Nature*, *401*(6755), 782–785.

Gvirtzman, Z., and A. Nur (2001), Residual topography, lithospheric structure, and sunken slabs in the central Mediterranean, *Earth Planet. Sci. Lett.*, *187*(1), 117–130.

Hacker, B. R., P. B. Kelemen, and M. D. Behn (2011), Differentiation of the continental crust by relamination, *Earth Planet. Sci. Lett.*, *307*(3–4), 501–516, doi:10.1016/j.epsl.2011.05.024.

Hattori, K. H., and S. Guillot (2007), Geochemical character of serpentinites associated with high- to ultrahigh-pressure metamorphic rocks in the Alps, Cuba, and the Himalayas: Recycling of elements in subduction zones, *Geochem. Geophys. Geosyst.*, *8*, Q09010, doi:10.1029/2007GC001594.

Hattori, K. H., S. Arai, and D. B. Clarke (2002), Selenium, tellurium, arsenic and antimony contents of primary mantle sulfides, *Can. Mineral.*, *40*(2), 637–650, doi:10.2113/gscanmin.40.2.637.

Hawkesworth, C., S. Turner, D. Peate, F. McDermott, and P. Van Calsteren (1997), Elemental U and Th variations in island arc rocks: Implications for U-series isotopes, *Chem. Geol.*, *139*(1), 207–221.

Hawkesworth, C. J., K. Gallagher, J. M. Hergt, and F. McDermott (1993), Mantle and Slab Contributions in ARC Magmas, *Annu. Rev. Earth Planet. Sci.*, *21*(1), 175–204, doi:10.1146/annurev.ea.21.050193.001135.

Hermann, J. (2002), Allanite: Thorium and light rare earth element carrier in subducted crust, *Chem. Geol.*, *192*(3–4), 289–306, doi:10.1016/S0009-2541(02)00222-X.

Hermann, J., and D. Rubatto (2009), Accessory phase control on the trace element signature of sediment melts in subduction zones, *Chem. Geol.*, *265*(3–4), 512–526, doi:10.1016/j.chemgeo.2009.05.018.

Hermann, J., C. Spandler, A. Hack, and A. V. Korsakov (2006), Aqueous fluids and hydrous melts in high-pressure and ultra-high pressure rocks: Implications for element transfer in subduction zones, *Lithos*, *92*(3–4), 399–417, doi:10.1016/j.lithos.2006.03.055.

Hofmann, A. W. (1997), Mantle geochemistry: The message from oceanic volcanism, *Nature*, *385*(6613), 219–229.

Ishikawa, T., and E. Nakamura (1994), Origin of the slab component in arc lavas from across-arc variation of B and Pb isotopes, *Nature*, *370*(6486), 205–208.

Ishikawa, T., and F. Tera (1997), Source, composition and distribution of the fluid in the Kurile mantle wedge: Constraints from across-arc variations of B/Nb and B isotopes, *Earth Planet. Sci. Lett.*, *152*(1–4), 123–138, doi:10.1016/S0012-821X(97)00144-1.

Ishikawa, T., and F. Tera (1999), Two isotopically distinct fluid components involved in the Mariana Arc: Evidence from Nb/B ratios and B, Sr, Nd, and Pb isotope systematics, *Geology*, *27*(1), 83–86.

Ishikawa, T., F. Tera, and T. Nakazawa (2001), Boron isotope and trace element systematics of the three volcanic zones in the Kamchatka arc, *Geochim. Cosmochim. Acta*, *65*(24), 4523–4537, doi:10.1016/S0016-7037(01)00765-7.

Johnson, M. C., and T. Plank (1999), Dehydration and melting experiments constrain the fate of subducted sediments, *Geochem. Geophys. Geosyst.*, *1*(12), 1007, doi:10.1029/1999GC000014.

Kawamoto, T., M. Kanzaki, K. Mibe, K. N. Matsukage, and S. Ono (2012), Separation of supercritical slab-fluids to form aqueous fluid and melt components in subduction zone magmatism, *Proc. Natl. Acad. Sci. U. S. A.*, *109*(46), 18,695–18,700, doi:10.1073/pnas.1207687109.

Kelemen, P. B., G. M. Yogodzinski, and D. W. Scholl (2003), Along-strike variation in the Aleutian island arc: Genesis of high Mg# andesite and implications for continental crust, in *Inside the Subduction Factory, Geophys. Monogr. Ser.*, vol.138, edited by J. Eiler, pp. 223–276, AGU, Washington, D. C.

Kelley, K. A., T. Plank, J. Ludden, and H. Staudigel (2003), Composition of altered oceanic crust at ODP Sites 801 and 1149, *Geochem. Geophys. Geosyst.*, *4*(6), 8910, doi:10.1029/2002GC000435.

Kessel, R., M. W. Schmidt, P. Ulmer, and T. Pettke (2005), Trace element signature of subduction-zone fluids, melts and supercritical liquids at 120-180 km depth, *Nature*, *437*(7059), 724–727, doi:10.1038/nature03971.

Kimura, J. I., and R. J. Stern (2008), Neogene volcanism of the Japan island arc: The Kh relationship revisited, Circum-Pacific Tectonics, Geologic Evolution, and Ore Deposits, *Ariz. Geol. Soc. Dig.*, *22*, 187–202.

Klimm, K., J. D. Blundy, and T. H. Green (2008), Trace element partitioning and accessory phase saturation during H2O-saturated melting of basalt with implications for subduction zone chemical fluxes, *J. Petrol.*, *49*(3), 523–553, doi:10.1093/petrology/egn001.

Krienitz, M. S., C. D. Garbe-Schonberg, R. L. Romer, A. Meixner, K. M. Haase, and N. A. Stroncik (2012), Lithium isotope variations in Ocean Island Basalts—Implications for the development of mantle heterogeneity, *J. Petrol.*, *53*(11), 2333–2347, doi:10.1093/petrology/egs052.

Kundu, B., and V. K. Gahalaut (2011), Slab detachment of subducted Indo-Australian plate beneath Sunda arc, Indonesia, *J. Earth Syst. Sci.*, *120*(2), 193–204.

Landi, P., L. Francalanci, M. Pompilio, M. Rosi, R. A. Corsaro, C. M. Petrone, I. Nardini, and L. Miraglia (2006), The December 2002–July 2003 effusive event at Stromboli volcano, Italy: Insights into the shallow plumbing system by petrochemical studies, *J. Volcanol. Geotherm. Res.*, *155*(3–4), 263–284, doi:10.1016/j.jvolgeores.2006.03.032.

Landi, P., R. A. Corsaro, L. Francalanci, L. Civetta, L. Miraglia, M. Pompilio, and R. Tesoro (2009), Magma dynamics during the 2007 Stromboli eruption (Aeolian Islands, Italy): Mineralogical, geochemical and isotopic data, *J. Volcanol. Geotherm. Res.*, *182*(3–4), 255–268, doi:10.1016/j.jvolgeores.2008.11.010.

Leeman, W. P. (1996), Boron and other fluid-mobile elements in volcanic arc lavas: Implications for subduction processes, in *Subduction Top to Bottom*, vol. 96, edited by G. E. Bebout, et al., pp. 269–276, AGU, Washington, D. C., doi:10.1029/GM096p0269.

Leeman, W. P., and V. B. Sisson (1996), Geochemistry of boron and its implications for crustal and mantle processes, in *Boron: Mineralogy, Petrology and Geochemistry in the Earth's Crust, Rev. Mineral.*, vol. 33, Min. Soc. Am., pp. 645–707.

London, D., and J. M. Evensen (2002), Beryllium in silicic magmas and the origin of beryl-bearing pegmatites, *Rev. Mineral. Geochem.*, *50*(1), 445–486, doi:10.2138/rmg.2002.50.11.

Lucchi, F., A. P. Santo, C. A. Tranne, A. Peccerillo, and J. Keller (2013a), Volcanism, magmatism, volcano-tectonics and sea-level fluctuations in the geological history of Filicudi (western Aeolian archipelago), *Geol. Soc. London Mem.*, *37*(1), 113–153, doi:10.1144/M37.8.

Lucchi, F., R. Gertisser, J. Keller, F. Forni, G. De Astis, and C. A. Tranne (2013b), Eruptive history and magmatic evolution of the island of Salina (central Aeolian archipelago), *Geol. Soc. London Mem.*, *37*(1), 155–211, doi:10.1144/M37.6.
Lucchi, F., A. Peccerillo, J. Keller, C. A. Tranne, and P. L. Rossi (2013c), The Aeolian Islands Volcanoes, *Geol. Soc. London Mem., 37*.
Lucchi, F., A. Peccerillo, C. A. Tranne, P. L. Rossi, M. L. Frezzotti, and C. Donati (2013d), Volcanism, calderas and magmas of the Alicudi composite volcano (western Aeolian archipelago), *Geol. Soc. London Mem.*, *37*(1), 83–111, doi:10.1144/M37.7.
Mallik, A., and R. Dasgupta (2013), Reactiveinfiltration of MORB-Eclogite-Derived carbonated silicate melt into fertile peridotite at 3 GPa and genesis of alkalic magmas, *J. Petrol.*, *54*(11), 2267–2300, doi:10.1093/petrology/egt047.
Mallik, A., J. Nelson, and R. Dasgupta (2015), Partial melting of fertile peridotite fluxed by hydrous rhyolitic melt at 2–3 GPa: Implications for mantle wedge hybridization by sediment melt and generation of ultrapotassic magmas in convergent margins, *Contrib. Mineral. Petrol.*, *169*(5), pp. 1–24, doi:10.1007/s00410-015-1139-2.
Mann, U., and M. W. Schmidt (2015), Melting of pelitic sediments at subarc depths: 1. Flux vs. fluid-absent melting and a parameterization of melt productivity, *Chem. Geol.*, *404*, 150–167, doi:10.1016/j.chemgeo.2015.02.032.
Manning, C. (2004), The chemistry of subduction-zone fluids, *Earth Planet. Sci. Lett.*, *223*(1–2), 1–16, doi:10.1016/j.epsl.2004.04.030.
Marschall, H. R., and J. C. Schumacher (2012), Arc magmas sourced from mélange diapirs in subduction zones, *Nat. Geosci.*, *5*(12), 862–867, doi:10.1038/ngeo1634.
Marschall, H. R., A. V. Korsakov, G. L. Luvizotto, L. Nasdala, and T. Ludwig (2009), On the occurrence and boron isotopic composition of tourmaline in (ultra)high-pressure metamorphic rocks, *J. Geol. Soc.*, *166*(4), 811–823, doi:10.1144/0016-76492008-042.
Martin, H., J.-F. Moyen, M. Guitreau, J. Blichert-Toft, and J.-L. Le Pennec (2014), Why Archaean TTG cannot be generated by MORB melting in subduction zones, *Lithos*, *198-199*, 1–13, doi:10.1016/j.lithos.2014.02.017.
Martindale, M., S. Skora, J. Pickles, T. Elliott, J. Blundy, and R. Avanzinelli (2013), High pressure phase relations of subducted volcaniclastic sediments from the west pacific and their implications for the geochemistry of Mariana arc magmas, *Chem. Geol.*, *342*, 94–109, doi:10.1016/j.chemgeo.2013.01.015.
Mazza, S. E., E. Gazel, E. A. Johnson, M. J. Kunk, R. McAleer, J. A. Spotila, M. Bizimis, and D. S. Coleman (2014), Volcanoes of the passive margin: The youngest magmatic event in eastern North America, *Geology*, *42*(6), 483–486, doi:10.1130/g35407.1.
Morris, J., J. Ryan, and W. P. Leeman (1993), Be isotope and B-Be investigations of the historic eruptions of Mt. Vesuvius, *J. Volcanol. Geotherm. Res.*, *58*(1), 345–358.
Morris, J. D., W. P. Leeman, and F. Tera (1990), The subducted component in island arc lavas: Constraints from Be isotopes and B-Be systematics, *Nature*, *344*(6261), 31–36.
Mullen, E. K., and D. Weis (2015), Evidence for trench-parallel mantle flow in the northern Cascade Arc from basalt geochemistry, *Earth Planet. Sci. Lett.*, *414*, 100–107, doi:10.1016/j.epsl.2015.01.010.
Neri, G., A. M. Marotta, B. Orecchio, D. Presti, C. Totaro, R. Barzaghi, and A. Borghi (2012), How lithospheric subduction changes along the Calabrian Arc in southern Italy: Geophysical evidences, *Int. J. Earth Sci.*, *101*(7), 1949–1969, doi:10.1007/s00531-012-0762-7.
Noll, P. D., H. E. Newsom, W. P. Leeman, and J. G. Ryan (1996), The role of hydrothermal fluids in the production of subduction zone magmas: Evidence from siderophile and chalcophile trace elements and boron, *Geochim. Cosmochim. Acta*, *60*(4), 587–611.
Panza, G. F., A. Aoudia, A. Pontevivo, G. Chimera, and R. Raykova (2003), The lithosphere-asthenosphere: Italy and surroundings, *Episodes*, *26*, 169–174.
Panza, G. F., A. Pontevivo, A. Sarao`, A. Aoudia, and A. Peccerillo (2004), Structure of the lithosphere–asthenosphere and volcanism in the Tyrrhenian Sea and surroundings, *Mem. Desc. Carta Geol. d'Italia*, *64*, 29–56.
Peccerillo, A. (2001), Geochemical similarities between the Vesuvius, phlegraean fields and Stromboli volcanoes: Petrogenetic, geodynamic and volcanological implications, *Mineral. Petrol.*, *73*(1–3), 93–105.
Peccerillo, A. (2005), *Plio-Quaternary Volcanism in Italy*, Springer, Berlin.
Peccerillo, A., and S. R. Taylor (1976), Geochemistry of Eocene calc-alkaline volcanic rocks from the Kastamonu area, northern Turkey, *Contrib. Mineral. Petrol.*, *58*(1), 63–81.
Peccerillo, A., and T. W. Wu (1992), Evolution of calc-alkaline magmas in continental arc volcanoes: Evidence from Alicudi, Aeolian arc (southern Tyrrhenian Sea, Italy), *J. Petrol.*, *33*(6), 1295–1315.
Peccerillo, A., P. D. Kempton, R. S. Harmon, T. W. Wu, A. P. Santo, A. J. Boyce, and A. Tripodo (1993), Petrological and geochemical characteristics of the Alicudi volcano, Aeolian Islands, Italy: Implications for magma genesis and evolution, *Acta Vulcanol.*, *3*, 235–249.
Peccerillo, A., L. Dallai, M. L. Frezzotti, and P. D. Kempton (2004), Sr–Nd–Pb–O isotopic evidence for decreasing crustal contamination with ongoing magma evolution at Alicudi volcano (Aeolian arc, Italy): Implications for style of magma-crust interaction and for mantle source compositions, *Lithos*, *78*(1–2), 217–233, doi:10.1016/j.lithos.2004.04.040.
Peccerillo, A., G. De Astis, D. Faraone, F. Forni, and M. L. Frezzotti (2013), Compositional variations of magmas in the Aeolian arc: Implications for petrogenesis and geodynamics, *Geol. Soc. London Mem.*, *37*(1), 491–510, doi:10.1144/M37.15.
Peccerillo, A., and M. L. Frezzotti (2015), Magmatism, mantle evolution and geodynamics at the converging plate margins of Italy, *J. Geol. Soc.*, *172*(4), 407–427, doi:10.1144/jgs2014-085.
Penniston-Dorland, S. C., G. E. Bebout, P. A. E. Pogge von Strandmann, T. Elliott, and S. S. Sorensen (2012), Lithium and its isotopes as tracers of subduction zone fluids and metasomatic processes: Evidence from the Catalina Schist, California, USA, *Geochim. Cosmochim. Acta*, *77*, 530–545, doi:10.1016/j.gca.2011.10.038.
Petrone, C. M., E. Braschi, and L. Francalanci (2009), Understanding the collapse–eruption link at Stromboli, Italy: A microanalytical study on the products of the recent Secche di Lazzaro phreatomagmatic activity, *J. Volcanol. Geotherm. Res.*, *188*(4), 315–332.
Pirard, C., and J. Hermann (2014), Experimentally determined stability of alkali amphibole in metasomatised dunite at sub-arc pressures, *Contrib. Mineral. Petrol.*, *169*(1), pp. 1–26, doi:10.1007/s00410-014-1095-2.
Piromallo, C., and A. Morelli (2003), Pwave tomography of the mantle under the Alpine-Mediterranean area, *J. Geophys. Res.*, *108*(B2), 2065, doi:10.1029/2002JB001757.
Plank, T. (2014), The chemical composition of subducting sediments, in *Treatise of Geochemistry*, 2nd ed., edited by E. Bebout, pp. 607–629, AGU, Washington, D. C., doi:10.1016/b978-0-08-095975-7.00319-3.
Plank, T., and C. H. Langmuir (1993), Tracing trace elements from sediment input to volcanic output at subduction zones, *Nature*, *362*(6422), 739–743.
Plank, T., and C. H. Langmuir (1998), The chemical composition of subducting sediment and its consequences for the crust and mantle, *Chem. Geol.*, *145*(3), 325–394.
Richards, S., G. Lister, and B. Kennett (2007), A slab in depth: Three-dimensional geometry and evolution of the Indo-Australian plate, *Geochem. Geophys. Geosyst.*, *8*, Q12003, doi:10.1029/2007GC001657.

Rottura, A., A. Del Moro, L. Pinarelli, R. Petrini, A. Peccerillo, A. Caggianelli, M. Bargossi, and G. Piccarreta (1991), Relationships between intermediate and acidic rocks in orogenic granitoid suites: Petrological, geochemical and isotopic (Sr, Nd, Pb) data from Capo Vaticano (southern Calabria, Italy), *Chem. Geol.*, *92*(1), 153–176.

Rudnick, R. L. (1995), Making continental crust, *Nature*, *378*(6557), 571–577.

Ryan, J., J. Morris, G. Bebout, and B. Leeman (1996), Describing chemical fluxes in subduction zones: Insights from "Depth-Profiling" studies of arc and forearc rocks, in *Subduction Top to Bottom*, pp. 263–268, American Geophysical Union.

Ryan, J. G. (2002), Trace-element systematics of Beryllium in terrestrial materials, *Rev. Mineral. Geochem.*, *50*(1), 121–145, doi:10.2138/rmg.2002.50.3.

Ryan, J. G., and C. Chauvel (2014), The subduction-zone filter and the impact of recycled materials on the evolution of the mantle, in *Treatise of Geochemistry*, 2nd ed., edited by E. Bebout, pp. 479–508, AGU, Washington, D. C., doi:10.1016/b978-0-08-095975-7.00211-4.

Ryan, J. G., and C. H. Langmuir (1988), Beryllium systematics in young volcanic rocks: Implications for 10Be*, *Geochim. Cosmochim. Acta*, *52*(1), 237–244, doi:10.1016/0016-7037(88)90073-7.

Ryan, J. G., and C. H. Langmuir (1993), The systematics of boron abundances in young volcanic rocks, *Geochim. Cosmochim. Acta*, *57*(7), 1489–1498.

Ryan, J. G., W. P. Leeman, J. D. Morris, and C. H. Langmuir (1996), The boron systematics of intraplate lavas: Implications for crust and mantle evolution, *Geochim. Cosmochim. Acta*, *60*(3), 415–422, doi:10.1016/0016-7037(95)00402-5.

Saginor, I., E. Gazel, C. Condie, and M. J. Carr (2013), Evolution of geochemical variations along the Central American volcanic front, *Geochem. Geophys. Geosyst.*, *14*, 4504–4522, doi:10.1002/ggge.20259.

Santo, A. P. (2000), Volcanological and geochemical evolution of Filicudi (Aeolian Islands, south Tyrrhenian Sea, Italy), *J. Volcanol. Geotherm. Res.*, *96*, 79–101.

Santo, A. P., S. B. Jacobsen, and J. Baker (2004), Evolution and genesis of calc-alkaline magmas at Filicudi Volcano, Aeolian Arc (Southern Tyrrhenian Sea, Italy), *Lithos*, *72*(1–2), 73–96, doi:10.1016/j.lithos.2003.08.005.

Savov, I. P., J. G. Ryan, M. D'Antonio, K. Kelley, and P. Mattie (2005), Geochemistry of serpentinized peridotites from the Mariana Forearc Conical Seamount, ODP Leg 125: Implications for the elemental recycling at subduction zones, *Geochem. Geophys. Geosyst.*, *6*, *Q04J15*, doi: 10.1029/2004GC000777.

Savov, I. P., J. G. Ryan, M. D'Antonio, and P. Fryer (2007), Shallow slab fluid release across and along the Mariana arc-basin system: Insights from geochemistry of serpentinized peridotites from the Mariana fore arc, *J. Geophys. Res.*, *112*, B09025, doi:10.1029/2006JB004749.

Scambelluri, M., and S. Tonarini (2012), Boron isotope evidence for shallow fluid transfer across subduction zones by serpentinized mantle, *Geology*, *40*(10), 907–910, doi:10.1130/G33233.1.

Schellart, W. P. (2008), Kinematics and flow patterns in deep mantle and upper mantle subduction models: Influence of the mantle depth and slab to mantle viscosity ratio, *Geochem. Geophys. Geosyst.*, *9*, Q03014, doi:10.1029/2007GC001656.

Schmidt, M. W., and S. Poli (1998), Experimentally based water budgets for dehydrating slabs and consequences for magma generation, *Earth Planet. Sci. Lett.*, *163*(1), 361–379.

Skora, S., and J. Blundy (2010), High-pressure hydrous phase relations of radiolarian clay and implications for the involvement of subducted sediment in arc magmatism, *J. Petrol.*, *51*(11), 2211–2243, doi:10.1093/petrology/egq054.

Skora, S., J. D. Blundy, R. A. Brooker, E. C. R. Green, J. C. M. de Hoog, and J. A. D. Connolly (2015), Hydrous phase relations and trace element partitioning behaviour in calcareous sediments at subduction-zone conditions, *J. Petrol.*, *56*(5), 953–980, doi:10.1093/petrology/egv024.

Spandler, C., and C. Pirard (2013), Element recycling from subducting slabs to arc crust: A review, *Lithos*, *170–171*, 208–223, doi:10.1016/j.lithos.2013.02.016.

Stegman, D. R., J. Freeman, W. P. Schellart, L. Moresi, and D. May (2006), Influence of trench width on subduction hinge retreat rates in 3-D models of slab rollback, *Geochem. Geophys. Geosyst.*, *7*, Q03012, doi:10.1029/2005GC001056.

Stolper, E., and S. Newman (1994), The role of water in the petrogenesis of Mariana trough magmas, *Earth Planet. Sci. Lett.*, *121*(3), 293–325, doi:10.1016/0012-821X(94)90074-4.

Straub, S. M., and G. D. Layne (2002), The systematics of boron isotopes in Izu arc front volcanic rocks, *Earth Planet. Sci. Lett.*, *198*(1), 25–39.

Syracuse, E. M., P. E. van Keken, and G. A. Abers (2010), The global range of subduction zone thermal models, *Phys. Earth Planet. Int.*, *183*(1–2), 73–90, doi:10.1016/j.pepi.2010.02.004.

Tatsumi, Y. (1989), Migration of fluid phases and genesis of basalt magmas in subduction zones, *J. Geophys. Res.*, *94*(B4), 4697–4707, doi:10.1029/JB094iB04p04697.

Tatsumi, Y., and S. Eggins (1995), *Subduction Zone Magmatism*, Blackwell Sci., Cambridge, Mass.

Tollstrup, D., J. Gill, A. Kent, D. Prinkey, R. Williams, Y. Tamura, and O. Ishizuka (2010), Across-arc geochemical trends in the Izu-Bonin arc: Contributions from the subducting slab, revisited, *Geochem. Geophys. Geosyst.*, *11*, Q01X10, doi: 10.1029/2009GC002847.

Tommasini, S., A. Heumann, R. Avanzinelli, and L. Francalanci (2007), The fate of high-angle dipping slabs in the subduction factory: An integrated trace element and radiogenic isotope (U, Th, Sr, Nd, Pb) study of Stromboli Volcano, Aeolian Arc, Italy, *J. Petrol.*, *48*(12), 2407–2430, doi:10.1093/petrology/egm066.

Tonarini, S., W. P. Leeman, and G. Ferrara (2001), Boron isotopic variations in lavas of the Aeolian volcanic arc, South Italy, *J. Volcanol. Geotherm. Res.*, *110*(1), 155–170.

Tonarini, S., S. Agostini, C. Doglioni, F. Innocenti, and P. Manetti (2007), Evidence for serpentinite fluid in convergent margin systems: The example of El Salvador (Central America) arc lavas, *Geochem. Geophys. Geosyst.*, *8*, Q09014, doi:10.1029/2006GC001508.

Tonarini, S., W. P. Leeman, and P. T. Leat (2011), Subduction erosion of forearc mantle wedge implicated in the genesis of the South Sandwich Island (SSI) arc: Evidence from boron isotope systematics, *Earth Planet. Sci. Lett.*, *301*(1–2), 275–284, doi:10.1016/j.epsl.2010.11.008.

Trua, T., G. Serri, and M. P. Marani (2003), Lateral flow of African mantle below the nearby Tyrrhenian plate: Geochemical evidence, *Terra Nova*, *15*(6), 433–440, doi:10.1046/j.1365-3121.2003.00509.x.

Trua, T., G. Serri, and P. L. Rossi (2004), Coexistence of IAB-type and OIB-type magmas in the southern Tyrrhenian back-arc basin: Evidence from recent seafloor sampling and geodynamics implications, *Mem. Desc. Carta Geol. d'Italia*, *44*, 83–96.

Trua, T., G. Serri, and M. Marani (2007), Geochemical features and geodynamic significance of the southern Tyrrhenian backarc basin, *Geol. Soc. Am. Spec. Pap.*, *418*, 221–233, doi:10.1130/2007.2418(11).

Trua, T., M. Marani, and F. Gamberi (2011), Magmatic evidence for African mantle propagation into the southern Tyrrhenian backarc region, *Geol. Soc. Am. Spec. Pap.*, *478*, 307–331, doi:10.1130/2011.2478(16).

Turner, S., B. Bourdon, and J. Gill (2003), Insights into magma genesis at convergent margins from U-series isotopes, *Rev. Mineral. Geochem.*, *52*(1), 255–315.

Turner, S., M. Handler, I. Bindeman, and K. Suzuki (2009), New insights into the origin of O–Hf–Os isotope signatures in arc lavas from Tonga–Kermadec, *Chem. Geol.*, *266*(3–4), 187–193, doi:10.1016/j.chemgeo.2009.05.027.

van Keken, P. E., B. R. Hacker, E. M. Syracuse, and G. A. Abers (2011), Subduction factory: 4. Depth-dependent flux of H2O from subducting slabs worldwide, *J. Geophys. Res.*, *116*, B01401, doi:10.1029/2010JB007922.

Ventura, G. (2013), Kinematics of the Aeolian volcanism (Southern Tyrrhenian Sea) from geophysical and geological data, *Geol. Soc. London Mem.*, *37*(1), 3–11, doi:10.1144/M37.2.

Voltaggio, M., M. Branca, D. Tedesco, P. Tuccimei, and L. Di Pietro (2004), 226Ra-excess during the 1631-1944 activity period of Vesuvius (Italy), *Geochim. Cosmochim. Acta*, *68*(1), 167–181, doi:10.1016/s0016-7037(03)00236-9.

Weldeab, S., K.-C. Emeis, C. Hemleben, and W. Siebel (2002), Provenance of lithogenic surface sediments and pathways of riverine suspended matter in the Eastern Mediterranean Sea: Evidence from 143Nd/144Nd and 87Sr/86Sr ratios, *Chem. Geol.*, *186*(1–2), 139–149, doi:10.1016/S0009-2541(01)00415-6.

White, W. M., and E. M. Klein (2014), Composition of the Oceanic Crust, in *Treatise of Geochemistry*, 2nd ed., edited by E. Bebout, pp. 457–496, AGU, Washington, D. C., doi: 10.1016/b978-0-08-095975-7.00315-6.

Whittaker, J. M., R. D. Müller, M. Sdrolias, and C. Heine (2007), Sunda-Java trench kinematics, slab window formation and overriding plate deformation since the Cretaceous, *Earth Planet. Sci. Lett.*, *255*(3–4), 445–457, doi:10.1016/j.epsl.2006.12.031.

Zimmer, M. M., T. Plank, E. H. Hauri, G. M. Yogodzinski, P. Stelling, J. Larsen, B. Singer, B. Jicha, C. Mandeville, and C. J. Nye (2010), The role of water in generating the calc-alkaline trend: New volatile data for Aleutian magmas and a new tholeiitic index, *J. Petrol.*, *51*(12), 2411–2444, doi:10.1093/petrology/egq062.

Zindler, A., and S. Hart (1986), Chemical geodynamics, *Annu. Rev. Earth Planet. Sci.*, *14*, 493–571.